Predicting Drought in the Green River Basin

Final Report

May 1, 2008

USGS-WWDC Water Research Program

Glenn Tootle (PI)

Steve Gray (Co-PI)

Thad Hunter (Graduate Research Assistant)

Tom Watson (Graduate Research Assistant)

Anthony Barnett (Graduate Research Assistant)

John Bellamy (Graduate Research Assistant)

University of Wyoming
Department of Civil and Architectural Engineering
1000 E. Univ. Ave.
Dept. 3295
Laramie, WY 82071-2000
tootleg@uwyo.edu
307-766-3299

Executive Summary and Research Results

On behalf of the graduate research assistants (Thad Hunter, Tom Watson, Anthony Barnett and John Bellamy), the Co-PI (Steve Gray) and the PI (Glenn Tootle), we hereby submit our final report *Predicting Drought in the Green River Basin*.

Chapter 1 addresses Task 1 (Evaluation of Streamflow Reconstruction Methodologies) and Task 4 (Improvement of Streamflow Reconstructions for the Green River Basin with New Tree-ring Collections) of the proposal. Anthony Barnett and Tom Watson were the lead investigators and authors of this chapter. Chapter 2 addresses Task 3 (Probabilistic Forecasting of Droughts) of the proposal. John Bellamy was the lead investigator and author of this chapter. Chapter 3 addresses Task 2 (Linkages of Streamflow with Large-Scale Ocean / Atmosphere Phenomena) of the proposal. Thad Hunter was the lead investigator and author of this chapter.

The research provided outstanding training and support for the above mentioned graduate students. Three of the four graduate students have completed their master's degree and are currently employed at engineering firms in the State of Wyoming. The fourth student will defend in Fall 2008.

The results of the research have been submitted to various peer-reviewed journals and as conference proceedings. This includes:

Hunter, T., Tootle, G.A., and T.C. Piechota, 2006. Oceanic-atmospheric variability and western U.S. snowfall. *Geophysical Research Letters*, 33, L13706.

Watson, T., F.A. Barnett, S. Gray and G. Tootle, 2008. Reconstructed Streamflow for the Headwaters of the Wind River, Wyoming USA. Submitted to *Journal of American Water Resources Association* (under 2nd review).

Barnett, F.A., T. Watson, S. Gray and G. Tootle, 2008. Upper Green River Basin Streamflow Reconstructions and Drought Analysis. Submittal pending to *Water Resources Research*.

Bellamy, J., G. Tootle, G. Kerr and L. Pochop, 2008. Frequency and Duration of Drought in the Green River Basin, WY, USA. Proceedings of the *ASCE World Water & Environmental Resources Congress 2008*, May 11-17, 2008, Honolulu, HI (In press).

In addition to numerous local presentations including the WY State Engineer's Water Forum and the University of Wyoming Graduate Seminars, numerous presentations were made at National and International Conferences including: 2006 ASCE EWRI Conference in Omaha, NE; 2007 AGU Conference in San Francisco, CA; 2008 AGU Hydrology Days in Ft. Collins, CO; and the upcoming 2008 ASCE EWRI Conference in Honolulu, HI.

The results of the research made several contributions including:

- The development of six new tree-ring chronologies for the Upper Green River Basin.

- The first successful streamflow reconstructions in the Upper Green River Basin. This includes streamflow reconstructions at major nodes used by the Bureau of Reclamation (BOR). BOR uses both instrumental and reconstructed streamflow in their Colorado River System Simulation System (CRSS) model. Also, headwaters gages were reconstructed which allowed for observing spatial variation in drought.

- The streamflow reconstructions revealed that significant "mega-droughts" have occurred. These mega-droughts far exceeded (in both length and magnitude) those droughts observed in the instrumental record. These results provide important information for water managers and planners.

- The magnitude, severity and risk of drought in the Upper Green River Basin were quantified and the recent (2000 to 2004) five year drought was examined. This resulted in the 2000 to 2004 drought having a frequency (probability of recurrence) of approximately 130 years.

- A distinct El Niño-Southern Oscillation (ENSO) was observed in streamflow and snowpack in the Wind River Range, including the Upper Green River Basin. A previous year summer La Niña (El Niño) results in increased (decreased) streamflow (or snowfall).

Table of Contents

Chapter 1 – Development of Upper Green River Basin Tree-Ring Chronologies and Streamflow Reconstructions

Abstract

The upper Green River represents a vital water supply for southwestern Wyoming and Upper / Lower Colorado River Compact states. Rapid development in the southwestern U.S. combined with the recent drought has greatly stressed the water supply of the Colorado River system and has increased interest in historic streamflows. The current research developed proxy records (streamflow) derived from tree ring chronologies in the Upper Green River Basin (UGRB). These streamflow reconstructions provide an effective way to analyze patterns of drought over a period of time extending beyond any instrumental record.

Nine streamflow reconstructions were developed for both headwaters stations (utilizing unimpaired streamflow records) and stations lower in the basin (utilizing naturalized streamflow records). Traditionally, streamflow reconstructions have mostly been limited to large rivers, but reconstructing headwaters records provides information to water users in the upper basin as well as providing spatial variability in streamflow throughout the river basin. In this study, all upper basin reconstructions extended back to the year 1615. The most downstream station in the UGRB (Green River near Greendale, UT) was extended to 1439 A.D. The coefficient of variance explained (R^2) for this reconstruction is 0.65.

Different modes of drought were identified within this reconstruction. Annual extremes (wet and dry) and persistent wet and dry (drought) periods were identified compared with long term trends in the reconstructed streamflow record.

Introduction

The Upper Green River Basin (UGRB, Figure 1) is a vital contributor to the Colorado River system, and the severity of the current multi-year drought has raised concerns about the ability of the upper basin states to meet obligations set fourth in the Colorado River Compact. Approximately thirteen percent of the available surface water in the Upper Colorado River Basin (UCRB) originates in the headwaters of the UGRB. The UGRB headwaters were one area of focus of the Lake Powell Research Project Bulletin, the first streamflow reconstruction effort based on information derived from tree rings (Stockton and Jacoby, 1976) and remain an area of interest for water planners within the Colorado River System (Brandon, 2005). In the three decades following the Stockton and Jacoby report, tree ring based research has been greatly improved by the addition of computer aided techniques and an increase in the number of available tree ring chronologies located within and adjacent to the Upper Colorado River Basin. The resulting improvement in streamflow proxy records has provided greater insight into the effects of severe sustained drought and the resulting economic impacts on water users within the Colorado River System (Lord et al., 1995; Young, 1995).

Recent reconstruction efforts have typically focused on streamflow gages at main nodes of the larger rivers (Woodhouse et al., 2006a; Meko et al., 2001; Cook and Jacoby, 1983) due to the larger area and population affected by potential streamflow deficits during periods of severe drought. Headwater stream reconstructions, in contrast, may not be representative of an entire basin but do provide information pertaining to inter-basin variability, and to water supplies in the

upper reaches of the given watershed (Woodhouse et al., 2006b; Woodhouse 2001). Ultimately, climate driven variations in streamflow affect all users from irrigators to individual domestic users. By examining long-term streamflow variations through dendrohydrological studies, a relative understanding of past, present, and future drought severity and duration can be obtained.

In order to create a network of streamflow proxies within the UGRB, two obstacles had to be overcome. First, there are many stream gaging stations in the UGRB but few have the required length and continuity in the instrumental record required to calibrate a streamflow reconstruction model. Second, few current tree ring chronologies are available in or adjacent to the UGRB.

Initially, the identification of serviceable stream gaging stations was performed, which resulted in nine spatially varied stations being selected. Next, six sites were selected for tree core collection in the foothills of the Wind River Mountain Range (on the eastern boundary of the UGRB, in Wyoming) that were used in the creation of six new tree ring chronologies (current to 2006). Two of the new chronologies were developed for sites sampled in the development of chronologies used for streamflow reconstructions in the UGRB (Stockton and Jacoby, 1976) and the original chronologies have since been employed in drought analysis in the UCRB (Meko et al., 1995). The addition of these six new chronologies to be used in conjunction with existing current chronologies (located in Wyoming, Colorado, and Utah) enables some tributary stream gages to be reconstructed for the first time in the UGRB. Also, the addition of these new chronologies provides information leading to more robust reconstructions of gages that have been reconstructed in the past (i.e. Green River at Warren Bridge and Green River at Green River, Wyoming).

Finally, the nine selected instrumental stream gages were reconstructed using the available tree ring chronologies in the region. Different modes of streamflow were examined in the streamflow proxy record developed for USGS gage #09234500 (Green River near Greendale, UT) which is located near the lower extent of the UGRB. Examination of these records shows extreme differences between flows in the instrumental and pre-instrumental periods, particularly in the duration and magnitude of droughts. These differences raise questions about how current management plans would address a severe sustained drought or wet period, as seen in reconstructed streamflow proxy records.

Study Area and Background
The UGRB has a watershed area of approximately 22,600 square miles and is located between the Wind River Mountain Range and the Wyoming Mountain Range in southwestern Wyoming. Winter snowpack is responsible for the majority of water year streamflow, which peaks during the spring-summer season (Mock, 1996). Due to the limited spring-summer season for peak streamflow, reservoir storage within the UGRB is designed to capture peak runoff allowing year-round distribution to the Colorado River System. The UGRB reservoir storage capacity is 4.36 million acre-feet in the ten largest reservoirs (Wyoming State Water Plan, 2007). This storage volume is over twice the average water year instrumental streamflow for the Green River near Greendale, Utah, near the lower extent of the UGRB. The storage capacity in the basin has allowed water managers and planners to mitigate the effects of drought events in the decades since the construction of the various dams.

Long-term hydroclimatic variability within individual river basins contributing to the Colorado River System has recently become an issue of greater interest given the current (1999 to present) drought. The UGRB headwaters were first studied as part of the Lake Powell Research Project Bulletin (Stockton and Jacoby, 1976), where headwater gage records as well as main stem river gage records were reconstructed (using tree ring data) to examine long-term variability in streamflow. In this 1976 report, three headwater gage reconstructions were successfully completed in the UGRB for the Green River, New Fork River, and North Piney Creek.

Although limited in scope, recent research has attempted to update and improve the Stockton and Jacoby (1976) UGRB results. The Palmer Drought Severity Index (PDSI) was reconstructed for the continental United States on a gridded network (Cook et al., 1999; Cook et al., 2004). However, the PDSI research did not provide information specific to inter-basin variability in the UGRB or provide any information directly pertaining to surface runoff.

Two projects directed at new and/or improved streamflow reconstructions include Woodhouse et al. (2006a) and Timilsena (2007). Woodhouse et al. (2006a) developed a reconstruction for the Green River near Green River, WY streamflow station and coefficient of variance of 0.48 was obtained for the reconstruction. This study relied heavily on tree ring chronologies from northern Colorado and Utah due to few updated chronologies being available in southwest Wyoming.

Timilsena (2007) attempted reconstructions at three gage locations in the UGRB including; Green River at Green River, WY, Green River at Warren Bridge, and East Fork River near Big Sandy, WY. This research demonstrated the need for an increased number of moisture sensitive tree ring chronologies in the region. For the Green River at Warren Bridge and East Fork River near Big Sandy, WY, Timilsena (2007) determined an insufficient number of predictors (i.e. tree ring chronologies) were available for the reconstruction regression model. Additionally, the Green River near Green River, WY reconstruction was unable to achieve a coefficient of variance of 0.40 (considered a minimum value for useful reconstructions) when utilizing tree ring chronologies available in the region.

Data and Methods
Streamflow Data
To create statistically robust streamflow reconstructions, it is necessary to use the most accurate streamflow information available for a given gage station. Therefore, unimpaired or naturalized streamflow data must be utilized to obtain true hydroclimatic variability (Slack et al., 1993). An unimpaired stream gage station is defined as a station with minimal effects of anthropogenic uses including storage, diversion, and consumptive use. The difference between unimpaired and naturalized streamflow is that naturalized flow is back calculated from an impaired gage record to represent a prehistoric flow at that station using information from unimpaired instrumental records higher in the watershed.

United States Geological Survey (USGS) stream gage information was obtained for all stream gages in the UGRB from the National Water Information System (NWIS) (http://waterdata.usgs.gov/nwis/sw). Although there are many gages in the UGRB, few have the continuous 40-50 year instrumental record necessary to calibrate a regression model while

remaining unimpaired. Unimpaired stations were identified using the Hydro-Climatic Data Network (HCDN)(Slack et al., 1993; Wallis et al., 1991). Of the gages meeting these criterion, six gages were selected for their spatial distribution within the UGRB and an additional three naturalized gages were added at three locations on the Green River. The naturalized data were provided by the United States Bureau of Reclamation (USBR) (Prairie, 2004) at river nodes used in the Colorado River Simulation System (CRSS). A total of nine gages were selected for reconstruction (Figure 1, Table 1).

Monthly streamflow data were converted to water year streamflow for all gage stations except Big Sandy River near Big Sandy, Wyoming (Q9). In the case of the Big Sandy River, March through September instrumental flow records were the only available data in the recent record. Cleaveland (2000), summer streamflow was reconstructed successfully using tree ring records, and in Watson et al. (2008) spring-summer streamflow was reconstructed for the Little Popo Agie River (a tributary to the Wind River). Results in Watson et al. (2008) showed that information vital to the local system could be obtained from reconstructed streamflow records at gage sites limited to spring-summer record.

Tree-Ring Chronologies
Tree ring data were obtained from multiple sources including the International Tree Ring Data Bank (ITRDB, 20 chronologies) (http://hurricane.ncdc.noaa.gov/pls/paleo/fm_createpages. treering), recent paleo-hydrological studies in regions surrounding the UGRB (9 chronologies) (Gray et al., 2004a; Gray et al., 2004b; Gray et al., 2007), and new tree ring collections (6 chronologies). The new tree ring chronologies were necessary to fill a spatial gap in existing chronology coverage within the headwater areas of the UGRB, along the Wind River Mountain Range. A total of 35 regional tree ring chronologies were considered in the UGRB streamflow reconstructions (Figure 1). Tree species used in these chronologies are considered moisture sensitive and include Douglas-fir (*Pseudotsuga menziesii*, PSME), piñon pine (*Pinus edulis*, PIED), limber pine (*Pinus flexilis*), and ponderosa pine (*Pinus ponderosa*, PIPO) (Fritts, 1976).

New Tree Ring Chronologies
Six new tree ring chronologies were developed from samples taken in the foothills of the Wind River Mountain Range. Three sampling sites were located within the UGRB, and an additional three sites were located (east across the continental divide) in adjacent river basins (Figure 1). Open stands of the available moisture sensitive species, Douglas-fir and limber pine, were sampled at elevations ranging from 6505 feet to 8610 feet. Sites were selected in areas having poorly developed and shallow soil, typically on rocky slopes, to minimize effects of persistent soil moisture (Fritts, 1976).

In an attempt to capture a broad spectrum of climatic variability, three Douglas-fir sites and three limber pine sites were sampled. Douglas-fir were sampled at one site near the southern terminus of the Wind River Mountain Range on Anderson Ridge (ARR), and at two sites on the southwest face of the Wind River Mountain Range near Boulder Lake (BLE) and near Fremont Lake (FMT). Limber pine were sampled at one site on the southwest face of the Wind River Mountain Range southeast of Fremont Lake (FSE) and two sites near the southern terminus of the Wind River Range, on the eastern end of Anderson Ridge (ARE) and near Red Canyon (RCU).

Trees were sampled using increment borers and a minimum of two cores were taken from each tree. After drying, the cores were glued to mounting blocks to preserve the samples. Cores were then progressively sanded and individual ring widths were measured with an accuracy of 0.001 mm. The resulting series were cross-dated using standard methods (Stokes and Smiley, 1968; Swetnam et al., 1985; Cook and Kairiukstis, 1990). The number of trees used in the new chronologies ranged from 20-35 trees and the number of core samples used in the new chronologies ranged from 28-70 samples (Table 2). Accuracy of the cross-dating procedure was verified using the COFECHA program (Holmes, 1983). COFECHA compares ring width measurements of a given series to measurements for the same year within the site, and provides statistics such as the overall inter-series correlation for a given site (Table 2).

Chronologies were created using the Auto-Regressive Standardization program (ARSTAN) (Cook, 1985; Cook and Kairiukstis, 1990). As employed here ARSTAN removes growth trends in individual tree ring series using a negative exponential or linear spline. The program then creates a chronology using a bi-weight robust mean approach, and outputs different chronology types; a chronology without detrended series (raw), a detrended chronology that is standardized to a value of one (standard), and a detrended residual chronology (residual). The residual chronology has low order autocorrelation that may be attributed to biological tree-growth factors removed (Fritts, 1976).

Since chronologies consist of two or more samples from 20-35 trees of differing ages, the number of samples typically decreases as the chronology extends back in time. The loss of sample depth can lead to shifts in variance (signal strength) in the early portions of the chronology. The subsample signal strength (SSS) statistic was assessed for each chronology throughout time (Wigley et al., 1984). A chronology cutoff point was established whereas the SSS statistic dropped below 0.85 (85% of the common variance is retained in the chronology of reduced sample depth when compared to the complete chronology), a threshold recommended in Wigley et al. (1984). Chronologies were abbreviated at the given cutoff before being used in streamflow reconstructions.

Pearson correlation values between the newly developed chronologies were significant at a 99% level (r = 0.32 to 0.80) and considered strong with the exception of RCU (Table 3). The new chronologies were also compared to others within the immediate region (r = 0.14 to 0.53) to determine if regional growth relationships exhibit continuity between individual tree ring-width indices. Evaluation of these inter-site relationships also provides an additional check of the cross-dating procedure performed in the creation of the new chronologies.

New Chronology Precipitation and Temperature Growth Linkages
Climate-growth relationships between the six new chronologies and different combinations of precipitation and temperature were evaluated by correlating instrumental climate records against both standard and residual chronologies. This procedure verifies the moisture sensitivity within each chronology (Fritts, 1976), and water-year precipitation emphasized, due to the goal of reconstructing water-year streamflow. Precipitation and temperature data were obtained for the surrounding climate divisions from the Western Regional Climate Center (http://www.wrcc.dri.edu). Climate-growth relationships were evaluated against individual climate stations in the region as well, but these stations were limited in length and continuity of

record.   Tree growth at five of the six new sites proved to be significantly correlated (95% level) to water-year precipitation. Ring-width growth was negatively correlated with climate division temperature records in all chronologies. Growth at RCU showed sensitivity to both precipitation and temperature but was not significantly correlated to either at a 95% level.

Reconstruction Procedure
Utilizing twenty nine existing tree ring chronologies and the six newly developed chronologies (35 total), regression models were calibrated to create reconstructions for the nine selected stream gage stations. Three standard regression techniques were assessed for the creation of these new reconstructions. Techniques included stepwise multiple linear regression (Woodhouse et al., 2006a), principal component regression (PCR, Hidalgo et al., 2000), and partial least squares regression (PLSR, Tootle et al., 2007). All tree ring predictors were subjected to a rigorous prescreening process (as described in 3.3.1) for use with specific instrumental stream gage records before being considered in the regression model for that station. Stepwise multiple linear regression was selected based on its wide acceptance in water resources and the similar skill obtained when compared to the other methods.

Preliminary reconstructions showed that the inclusion of chronologies from the region surrounding the UGRB improved the statistical strength of the streamflow reconstructions. This was most likely due to the lack of usable inter-basin chronologies. The addition of regional chronologies can provide more complete information pertaining to climatic variability observed in the tributary drainage basin (Gedalof et al., 2004; Cook et al., 1999, 2004; Watson et al., 2008). Reconstruction models using out of basin chronologies were statistically evaluated against a model calibrated with only inter-basin chronologies to verify statistical improvement, and this was attributed to the general lack of inter-basin chronologies.

Prescreening of Predictors
When comparing low order autocorrelation displayed in the nine instrumental stream gage records (r = -0.06-0.23, Table 1) to autocorrelation in both the standard chronologies (r = 0.46-0.55) and the residual chronologies (r = 0.00-0.01) it is evident that streamflow will be more accurately represented by the residual chronologies. Therefore, residual chronologies were considered in the regression model for each of the nine gage stations and were selected from the original pool of thirty five tree ring chronologies (predictors) using two methods in succession. First, only chronologies exhibiting 30% of the variability observed in the instrumental streamflow record (R ≥ 0.30) that were 99% significantly correlated (p < 0.01) were considered. The retained chronologies were then subjected to bootstrapped correlation using evolutionary and moving intervals applying DENDROCLIM2002 (Biondi et al., 2004), a program designed to test stability in the relationship between the predictor and the hydroclimatic variable. Forward and backward evolutionary windows were evaluated for various base lengths and predictors that maintained stable correlations over time were retained in the pool of predictors for each stream gage reconstruction model.

Stepwise Multiple Linear Regression and Validation Statistics
Stepwise multiple linear regression was utilized to create reconstructed streamflow proxy records for the nine instrumental gage stations selected. A forward and backward stepwise reconstruction process entered and removed predictors with a threshold F value of 4 (Draper and

Smith, 1998). The F value is a measurement of the difference between individual distributions and the confidence of the difference (i.e. as F values increase, p values decrease). The predictor with the highest partial F value is entered into the model first with additional predictors being individually entered if the addition is significant (F greater than 4) in the regression equation. Likewise, if retaining a predictor is not significant (F less than 4) in the regression equation it will be removed. The statistical strength and fit of the resulting regression models are summarized by the following statistics: R^2, R^2(adjusted), R^2(predicted), F statistic, root mean square error (RMSE; Weisberg, 1980), cross validation standard error (CVSE, Garen, 1992), variance inflation factor (VIF; Haan, 2002), Mallows' C-p (Weisberg, 1980), the predicted error sum of squares (PRESS; Maidment, 1993), and the Durbin-Watson statistic (Draper and Smith, 1998).

The regression models were evaluated using two validation techniques. A regression model was first calibrated on the first half of the data and validated on the second half of the data. This procedure is then reversed by calibrating on the second half of the data and validated on the first half. A second more robust approach, leave-one-out cross validation, was also applied (Michaelsen, 1987). Leave-one-out cross validation creates a validation series by dropping each year, creating a regression equation, and then predicting a value for the dropped year. The original regression model is then validated against the leave-one-out validation series.

Integrating Gage and Reconstructed Records
Ideally, the variance observed in historic stream gage record will be equal to the variance observed in the reconstruction calibration period. Depending on the observed variance explained in the reconstructed time series, this may not be the case. To remedy this discrepancy in standard deviation, a conservative approach described in Timilsena et al. (2007) was employed. This method rescales reconstructed streamflow values to force the standard deviation in the reconstructed record to be equal to the standard deviation observed in stream gage record using:

$$\hat{x}_a = \left(\frac{\hat{x}_i - \bar{\hat{x}}}{\hat{\sigma}} \right) \sigma + \bar{\hat{x}}$$

where, $\hat{x}_i$ is the initial reconstructed variable, $\bar{\hat{x}}$ is the mean of the entire reconstructed time series, $\hat{\sigma}$ is the standard deviation of the entire reconstructed time series, σ is the standard deviation observed in the gage record used in model calibration, and $\hat{x}_a$ is the adjusted reconstructed variable.

Performing this adjustment allows the stream gage record to be joined with the reconstructed time series. This integration is necessary when using chronologies in the regression model that are not as current as available stream gage record and to retain as much current information as possible for analysis. All reconstructions were adjusted using this procedure to integrate available gage record.

Analysis of Reconstructed Wet and Dry Periods
A comprehensive analysis of wet and dry periods was completed for the Green River near Greendale, UT reconstruction. The first analysis compares these streamflow reconstructions to a precipitation reconstruction from northeastern Utah (Gray et al., 2004b). This comparison focused on extreme (above the ninety fifth quantile and below the fifth quantile) wet and dry

years in the reconstruction. Next, five year periods of persistent severe wet and dry conditions were examined by setting a threshold for wet water year values as the third quartile and the threshold for dry water year values as the first quartile.

Significant wet and dry periods were identified by applying confidence bands to reconstructed values at a 95% significance level. The confidence bands are based on the RMSE estimate from the calibration period of the reconstruction (Jain et al., 2002). If the mean streamflow for the reconstruction falls within the confidence band of plus or minus two times the RMSE for any reconstructed value, the reconstructed value is assumed not to be a significant event and the mean value of for the reconstruction is inserted in place of the reconstructed value. To examine long term variability in streamflow, a twenty five year filter (centered) was applied to an extended version (1439 to 2004) of the Greendale, UT reconstruction.

Streamflow Reconstruction Analysis (Results and Discussion)
Streamflow reconstructions were completed for the nine gages identified as having adequate continuous instrumental gage record for calibration.   The Green River near Greendale, UT (Q1) gage station, the most downstream station in the UGRB, was a focal point of the analysis since it encompasses streamflow contributions for the entire UGRB (Figure 2). Correlations between the Green River near Greendale, UT reconstruction and other reconstructed gage records in the UGRB were relatively high   (R = 0.73–0.96). Statistical evaluation of all reconstructed streamflow records shows a general trend of increasing explained variance from the upper reaches of the basin to the basin outlet (Table 4).

Streamflow Reconstructions
The regression model for Green River near Greendale, UT incorporated six tree ring chronologies extending back to 1615 A.D. (or earlier). The model was calibrated from 82 years of naturalized gage record (1914-1995). The full naturalized gage record (1905-2004) was not used due to few operational gage stations being available in the UGRB during the early years of the naturalized record and not all of the chronologies selected for the regression analysis were current (to 2006). A set of descriptive statistics were developed to describe and validate the final reconstruction model (Table 4), which captured sixty five percent of the observed variance in the gage record (Figure 3).

Collectively, statistics testing the strength and fit of the Green River near Greendale, UT reconstructions were strong. Analysis showed little variance inflation added by any predictors within the model (i.e., VIF not significantly greater than 1), and the Durbin-Watson statistic revealed little autocorrelation within predictors included in the model. Cross validation of the regression model verifies that total variance explained (R^2) is not exaggerated by the regression model since the R^2 (predicted) from the leave-one-out cross validation technique is not significantly less than the overall R^2. The RMSE and CVSE calculated for the calibration period were smaller than one standard deviation. The Green River Greendale, UT reconstruction (Figure 4) displays well-known droughts in 1930's and 1950's as well as wet periods in the 1920's and 1980's.

Headwater Reconstructions

Six streamflow reconstructions were completed for headwater gage stations. The total variance explained in the headwaters gage reconstructions ranged from 0.44-0.58 (Table 4). The regional (spatial) variation in reconstructed UGRB headwater gages can be identified by correlating the reconstructed records or by visual inspection (Figure 5). Correlation values range from 0.67-0.98 for the reconstructed headwater gages (Table 5). Similarities in the reconstructed headwater records may in part be attributed to the use of many of the same tree ring chronologies in the individual regression models.

When rescaling the reconstructed record to incorporate the instrumental gage record at three headwater gages, negative values for water year streamflow were observed. The stations where negative values were observed had relatively short calibration periods that did not include the severe drought of the 1930's. Integrating the gage record into the reconstructed record provides a comparison for water managers and planners between current drought events and events observed in the reconstructed historic record, but values can only be evaluated on a relative scale.

CRSS Node Reconstructions

Three statistically robust reconstructions of CRSS node gage stations were completed. Similar to the reconstructed headwater gages, the reconstructed records for the three nodes on the main stem of the Green River are highly correlated. In both naturalized records and reconstructed records, correlation of the Green River near Green River, WY (Q2) and the Green River below Fontenelle Reservoir (Q3) show the two gage stations behave the same throughout time. The addition of tributary streamflow lower in the UGRB results in variation in the streamflow for the Green River near Greendale, UT (Q1). This variation is evident by visual inspection (Figure 6), when compared to the other two CRSS nodes, but correlation values remain high (R > 0.95).

Extended Greendale Reconstruction

A second, extended, reconstruction was completed for the Green River near Greendale, UT (Q1) gage station to examine long term changes in streamflow. Only one tree ring chronology from within the UGRB was utilized since no other chronologies passing the prescreening requirements extended back before 1603 A.D. (Table 2), the year in which a cutoff point was established for the new chronology at Fremont Lake (FMT). Using extended chronologies in the region, a reconstruction achieving fifty percent of the variance observed in the instrumental record was completed. When applying the paired t-test the extended reconstruction (1439-1999) was not statistically similar (p<0.05) to the original reconstruction (1615-1999) of water year streamflow for the overlapping period of record. However, when a ten year filter was applied to both reconstructions, a visual analysis reveals possible usefulness of the extended reconstruction in an evaluation of long term changes in reconstructed streamflow (Figure 7).

Summary of Reconstructed Streamflow Characteristics

Comparing the newly developed UGRB streamflow reconstructions with other reconstructions in the region shows relative similarity in values of explained variance (i.e., Front Range and Upper Colorado River Basin reconstructions (R^2=0.63-0.76) per Woodhouse et al., 2006b and Yellowstone River (R^2=0.52) per Graumlich et al., 2003). Previously reconstructed stations and first time reconstructions have been improved or enabled by the addition of new tree ring chronologies and longer calibration periods. The Green River at Warren Bridge, near Daniel,

WY was previously reconstructed by Stockton and Jacoby (1976), and the variance explained was improved from 0.41 to 0.44. The Green River near Green River, WY was reconstructed by Woodhouse et al. (2006a) and the variance explained was improved from 0.48 to 0.60.

A comparison of instrumental and reconstructed gage records for the nine selected gages in the UGRB show increased variability (between minimum and maximum flows) in water year streamflow in the reconstructed records when compared to the instrumental records (Table 6). This comparison shows that the 20th century instrumental streamflow records alone do not provide a sufficient base of information for water managers and planners to fully understand historic streamflow regimes. Combining instrumental gage records with reconstructed records can provide greater insight into possible periods of future drought and above average streamflow. It should be noted that the standard deviation of the instrumental gage record is greater than the standard deviation of the reconstructed record without applying the rescaling method (described in section 3.4). By rescaling the reconstructed records, standard deviations are forced to be equal.

Drought and Wet Periods Observed in Greendale, UT Reconstruction
Reconstructed flows within the streamflow proxy for the Green River at Greendale, UT capture wet years (i.e. 1917, 1983, and 1986) and dry years (i.e. 1934 and 1977) observed in the instrumental gage record. Comparisons with the Gray et al. (2004b) precipitation study show that pre-instrumental wet years (e.g. 1680 and 1701) and dry years (e.g. 1685, 1735, 1756, 1773, and 1871) in the reconstructions are similar. The analysis of consecutive wet and dry years revealed only one five-year run of deficit streamflow. This period is notable since it occurred during the current drought (i.e. 2000-2004).

Significant Water Year Events
An examination of streamflow events either exceeding the 95th quantile or failing to exceed the fifth quantile reveals the relative wetness of the 20th Century. Seven of the twenty two individual water-year streamflow values exceeding the ninety-fifth quantile are within the 20th Century and only two of the twenty one individual water year streamflow values failing to exceed the fifth quantile occur within the same period of time (Figure 8). The two water-year values failing to exceed the fifth quantile (i.e. 1934 and 1977) were within the instrumental gage record.

Long Term Streamflow Variability
Evaluation of wet and dry periods throughout the extended streamflow reconstruction again reveals the 20th Century as being wetter than average. The twenty five year cubic spline used to analyze the wet to dry phase changes was validated by plotting it with all water year values considered to be significantly wet or dry (Figure 9). The trend of the spline followed patterns seen in the significantly wet or dry values with greater magnitudes in areas of dense clusters of values significantly deviating from average.

The analysis of the twenty five year moving average reveals another unique scenario pertaining to water management and planning. Within any given 25- year period varies above and below the mean value of streamflow, but the period as a whole is typically skewed towards wet or dry (Figure 10). One evident period of severe sustained drought is the 16th Century "Mega Drought" (Stahle et al., 2000), and is displayed in nearly all tree ring based reconstructions in the western

United States (e.g., Stockton and Jacoby, 1976 and Woodhouse et al., 2006a). The instrumental gage record alone does not display any of these extended shifts toward either the wet or dry side of average, but does display one of the wettest periods in the entire record. Comparing the instrumental mean to the mean of the entire reconstructed record shows how wet the 20th Century has been (Figure 10, Figure 11). If a threshold for surplus / deficit streamflow is set at the instrumental mean, it would appear that periods of drought have been the dominate trend in historic streamflow. Setting the threshold at the mean of the entire reconstructed record shows that duration and magnitude vary in both wet and dry periods, but distribution of these events are relatively even.

Summary and Conclusions

The addition of six new tree ring chronologies enabled the creation of nine new or updated streamflow proxy records in the UGRB. Three of the gages for which reconstructions were completed are important forecasting points in the Upper Colorado River Basin (CRSS nodes). The addition of the CRSS node proxies are important in understanding the contribution to the Colorado River System provided by the UGRB. The UGRB has been shown to be one of the controlling subbasins (e.g. severe droughts in the UGRB such as the 1930's outweighed the effects of higher flows from the San Juan River Basin in historic records for Lees Ferry, AZ) in the Upper Colorado River Basin (Woodhouse et al., 2006a). Streamflow proxy records developed for headwater stream gages were similar to the proxies developed for the CRSS nodes and identified periods of extreme drought apparent in all reconstructed proxy records.

All streamflow proxies developed in the research show the 20th Century to be noticeably wetter than previous centuries. While periods of drought observed in the 1930's and 1950's severely impacted water users in the UGRB, it is likely these droughts have been exceeded by events occurring prior to instrumental stream gage records. The historic approximation of streamflow derived from tree ring records provides pertinent information to water managers when planning for future events by examining historic variations in streamflow. Using these pre-instrumental records, climatic teleconnections may be identified and drought frequency / duration analysis may provide water planners and managers with appropriate tools to better plan for future availability.

References

Biondi, F. and K. Waikul (2004), DENDROCLIM2002: A C++ program for statistical calibration of climate signals in tree-ring chronologies. Computers & Geosciences 30: 303-311.

Brandon, D. (2005), Using NWSRFS ESP for making early outlooks of seasonal runoff volumes into Lake Powell, Print at the special session of the AMS annual meeting, hydrology of arid and semi-arid regions, San Diego, CA.

Cleaveland M.K. (2000), A 963-year reconstruction of summer (JJA) streamflow in White River, Arkansas, USA, from tree-rings, The Holocene, 10(1):33-41.

Cook, E.R. (1985), A time series approach to tree-ring standardization, Ph.D. dissertation, Univ. of Ariz., Tucson.

Cook, E.R., C.A. Woodhouse, C.M. Eakin, D.M. Meko, and D.W. Stahle (2004), Long-term aridity changes in the western United States, *Science*, 306, 1015-1018

Cook E.R. and G.C. Jacoby (1983), Potomac River streamflow since 1730 as reconstructed by tree rings, Journal of Climate and Applied Meteorology, 22(10): 1659-1672.

Cook, E.R., and L.A Kairiukstis (1990), *Methods of Dendrochronology: Applications in the Environmental Sciences*, Kluwer Academic Publishers and International Institute for Applied System Analysis, Dordrecht, The Netherlands.

Cook, E.R., D.M. Meko, D.W. Stahle, and M.K. Cleaveland (1999), Drought reconstructions for the continental United States, Journal of Climate 12, 1145-1162.

Draper, N.R., and H. Smith (1998), Applied Regression Analysis. Third Ed. Wiley, New York, p. 69 & 330-346.

Fritts, H.C. (1976), Tree Rings and Climate, Academic Press, London, United Kingdom.

Garen, D.C. (1992), Improved techniques in regression-based streamflow volume forecasting. Journal of Water Resources Planning and Management, 118:654-670

Gedalof, Z., D.L. Peterson, and N.J. Mantua (2004), Columbia River flow and drought since 1750. Journal of the American Water Resources Association (JAWRA) 40(6): 1579-1592.

Graumlich, L.J., M.F.J. Pisaric, L.A. Waggoner, J.S. Littell, and J.C. King (2003), Upper Yellowstone River flow and teleconnections with Pacific Basin climate variability during the past three centuries, Climatic Change, 59 (1-2):245-262.

Gray, S.T., C. Fastie, S.T. Jackson, and J.L. Betancourt (2004a), Tree-ring based reconstructions of precipitation in the bighorn Basin, Wyoming since AD 1260. Journal of Climate, 17, 3855-3865.

Gray, S.T., S.T. Jackson, and J.L. Betancourt (2004b), Tree-ring based reconstructions of interannual to decadal-scale precipitation variability for northeastern Utah, J. Am. Water Resour. Assoc., 40, 947-960.

Gray, S.T., L.J. Graumlich, and J.L. Betancourt (2007), Annual precipitation in the Yellowstone National Park region since AD 1173, Quaternary Research, doi:10.1016/j.yqres.2007.02.002.

Haan, C.T. (2002), Statistical Methods in Hydrology, 2nd ed. Iowa State Univ. Press, Ames, Iowa. 378 pp.

Hidalgo, H.G., T.C. Piechota, and J.A. Dracup (2000), Streamflow reconstruction using alternative PCA-based regression procedures, Water Resources Research, 36(11): 3241-3249.

Holmes, R.L. (1983), Computer-assisted quality control in tree-ring dating and measurement. Tree-Ring Bulletin 43:69-95.

ITRDB (International Tree Ring Data Bank) (2007), Tree-ring data search, available at http://hurricane.ncdc.noaa.gov/pls/paleo/fm_createpages.treering, Accessed November, 2007.

Jain, S., Woodhouse, C. A., Hoerling, M. P. (2002), Multidecadal streamflow regimes in the interior western United States: Implications for the vulnerability of water resources. Geophysical Research Letters, 29(21), 2036, doi:10.1029/2001GL014278.

Lord, W. B., Booker, J. F., Getches, D. M., Harding, B. L., Kenney, D. S., Young, R. A. (1995), Managing the Colorado River in a severe sustained drought: An evaluation of institutional options, Water Resources Bulletin, 31(6), 939-944.

Maidment, D.R. ed. (1993), Handbook of Hydrology. McGraw-Hill, Inc. New York, 17.42, 19.20.

Meko, D.M., C.W. Stockton and W.R. Boggess (1995), The tree-ring record of severe sustained drought. Water Resources Bulletin, 31(5):789-801.

Meko, D.M., M.D. Therrell, C.H. Baisan, and M.K. Hughes (2001), Sacramento River flow reconstructed to A.D. 869 from tree rings', Journal of American Water Resources Assoc. 37, 1029-1039.

Michealson, J. (1987), Cross validation in statistical climate forecast models, Journal of Applied Meteorology. 26(11): 1589-1600.

Mock, C.J. (1996). Climatic Controls and Spatial Variations of Precipitation in the Western United States. J. Climate 9:1111-1125.

NWIS (National Water Information System) (2007), USGS surface-water data for the nation, available at http://waterdata.usgs.gov/nwis/sw, Accessed November, 2007.

Prairie, J (2004), Naturalized flows 1906-2004 for the Colorado River Basin, U.S. Bureau of Reclamation.

Slack, J. R., A. Lumb, and J. M. Landwehr (1993), Hydro-Climatic Data Network (HCDN) Streamflow Data Set, 1874-1998. CD-ROM. U.S. Geological Survey, Reston, Virginia, U.S.A. Available from Oak Ridge National Laboratory Distributed Active Archive Center, Oak Ridge, Tennessee, U.S.A. [http://www.daac.ornl.gov].

Stahle, D.W., E.R. Cook, M.K.Cleaveland, M.D. Therrell, D.M. Meko, H.D. Grissino-Mayer, E. Watson, and B.H. Luckman (2000), Tree-ring data document 16th century megadrought over North America, Eos Trans. AGU, 81(12), 121,125.

Stockton, C.W., and G.C. Jacoby (1976), Long-term surface water supply and streamflow trends in the Upper Colorado River Basin, Lake Powell Research Project Bulletin No. 18, Nation Science Foundation, Arlington, VA

Stokes, M.A., and T.L. Smiley (1968), *An Introduction to Tree-Ring Dating*, Univ. of Ariz. Press, Tucson.

Swetnam, T.W., M.A. Thompson, and E.K. Sutherland (1985), *Using Dendrochronology to Measure Radial Growth of Defoliated Trees*, Agric. Handb., vol. 639, For. Serv., U.S. Dep. Of Agric., Washington, D.C.

Timilsena, J. (2007), Reconstruction of hydrologic and climatic variability in the Colorado River Basin, Ph.D. dissertation, Univ. of Nevada., Las Vegas.

Timilsena, J., T. C. Piechota, H. G. Hidalgo, and G. Tootle (2007), Five hundreds years of drought in the Upper Colorado River Basin. Journal of American Water Resources Association. 43(3):798-812.

Tootle, G.A., A.K. Singh, T.C. Piechota, and I. Farnham (2007), Long Lead-Time Forecasting of U.S. Streamflow Using Partial Least Squares Regression. Journal of Hydrologic Engineering, ASCE, 1084-0699, 12:15(442).

Wallis, J. R., Lettenmaier, D.P., and Wood, E. F. (1991). A daily hydro-climatical data set for the continental United States, Water Resources Research, 27(7), 1657-1663.

Watson, T., F.A. Barnett, S. Gray and G. Tootle (2008). Reconstructed Streamflow for the Headwaters of the Wind River, Wyoming USA. Submitted to *Journal of American Water Resources Association* (under 1st review).

Weisberg, S. (1980), *Applied Linear Regression*, John Wiley & Sons, New York, N.Y

Wigley, T., K. Briffa, and P.D. Jones (1984), On the average value of correlated time series, with applications in dendroclimatology and hydrometeorology, J. Clim. Appl. Meteorol., 23, 201-213.

Woodhouse, C.A. (2001). A tree-ring reconstruction of streamflow for the Colorado Front Range. J. American Water Resources Association (JAWRA) 37:561-569.

Woodhouse, C. A. and Lukas, J.J. (2006b), Multi-century tree-ring reconstructions of Colorado streamflow for water resource planning, Climate Change, 78:293-315, doi: 10.1007/s10584-006-9055-0.

Woodhouse, C.A., S.T. Gray, and D.M. Meko (2006), Updated streamflow reconstructions for the Upper Colorado River Basin, Water Resour. Res., 42, W05415, doi:10.1029/2005WR004455.

WRCC (Western Regional Climate Center) (2007), Historical climate information, available at http://www.wrcc.dri.edu, Accessed November, 2007.

Wyoming State Water Plan (1970), Green River Basin water plan technical memoranda, http://waterplan.state.wy.us/plan/green/techmemos/reservoir.html. Accessed November 2007.

Young, R. A. (1995), Coping with a severe sustained drought on the Colorado River: Introduction and overview, Water Resources Bulletin, 31(6), 779-788.
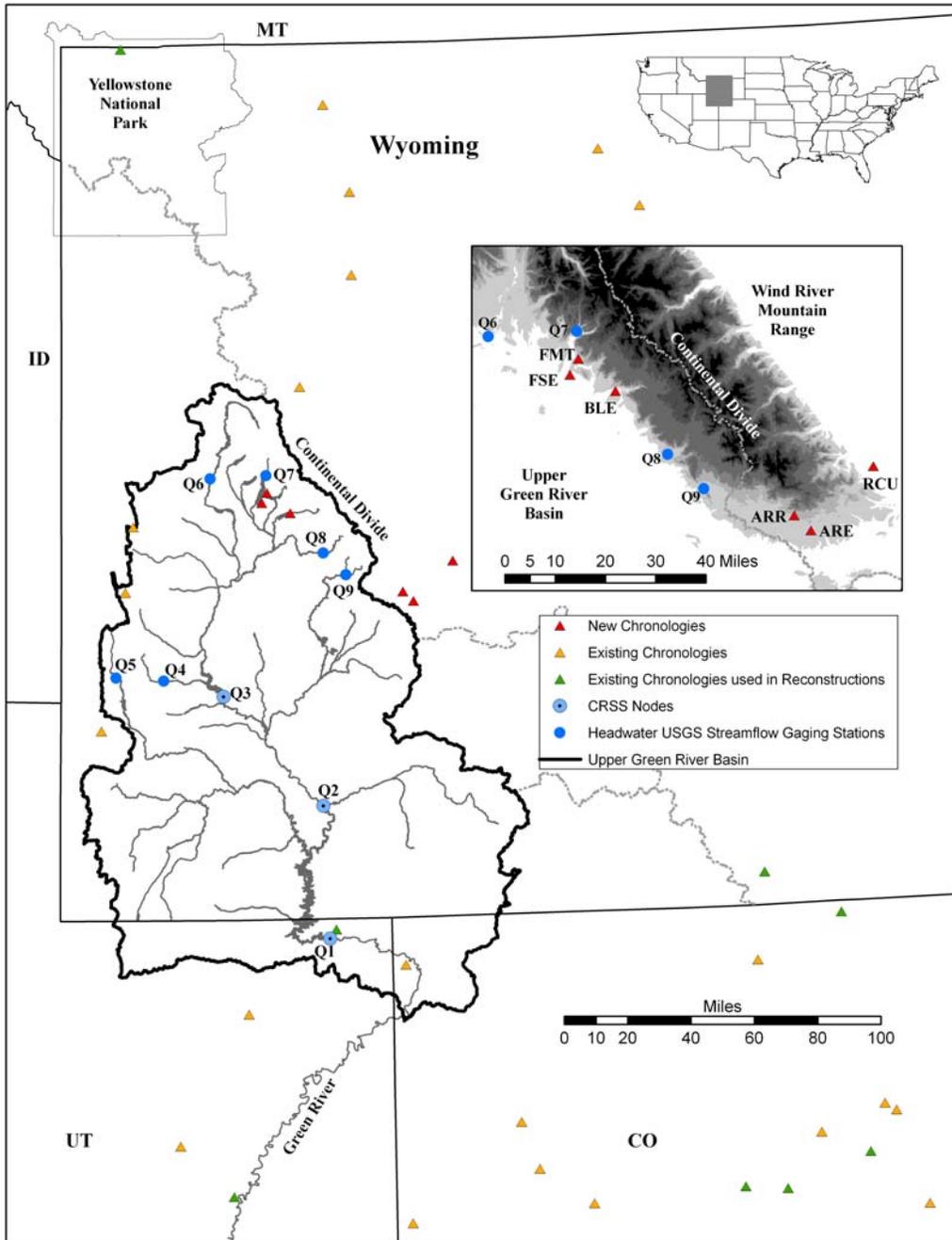
Figure 1: Map of Study area
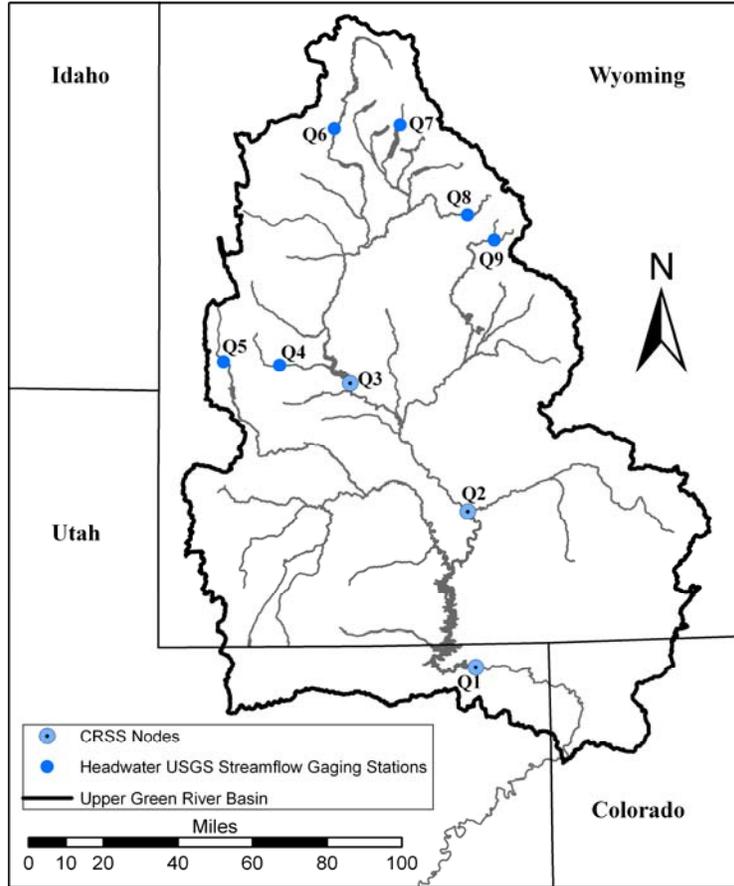
Figure 2: Location of reconstructed UGRB stream gage stations.
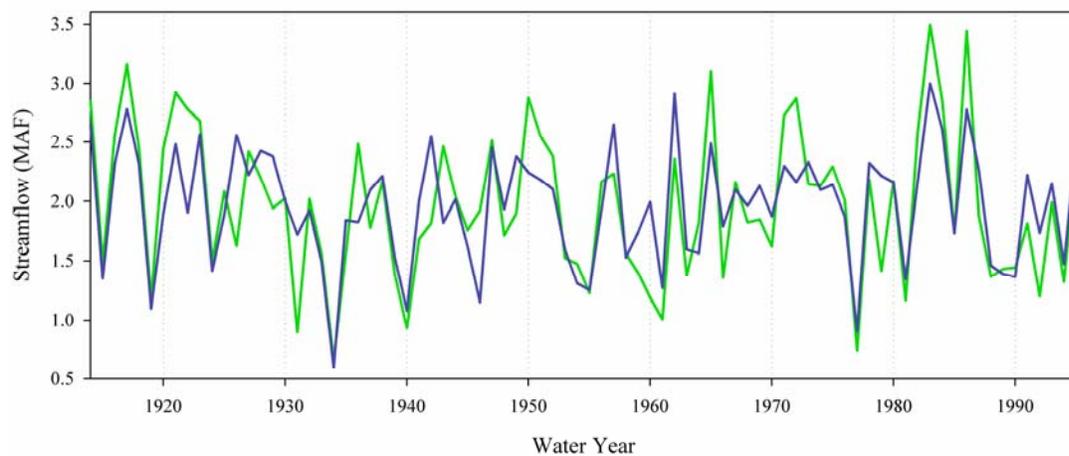
Figure 3: Comparison of observed (blue line) and reconstructed (green line) streamflow for the Green River near Greendale, UT for the calibration period.
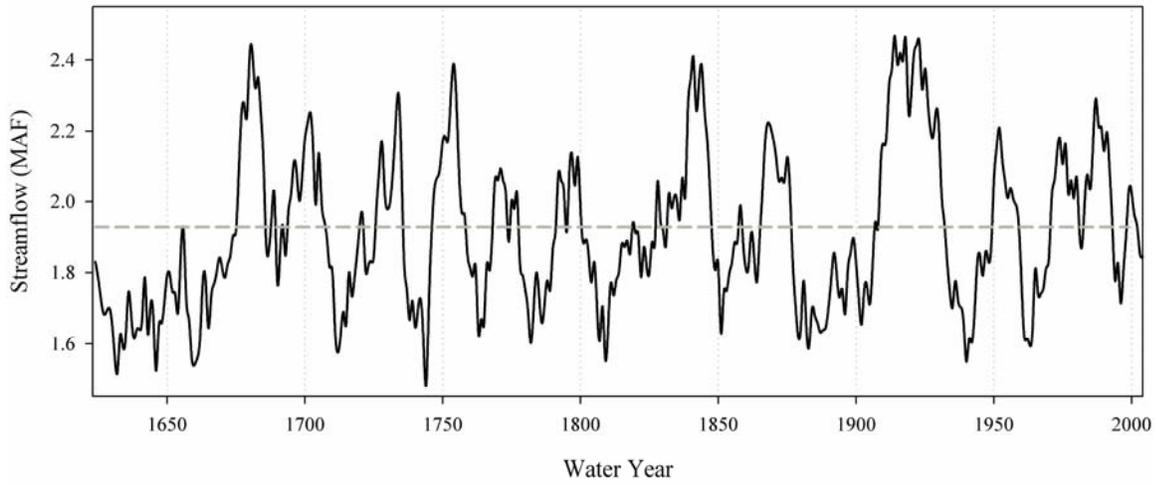
Figure 4: Reconstructed streamflow (black line) with ten year filter (end year displayed) and mean reconstructed flow (grey line) for the Green River near Greendale, UT.
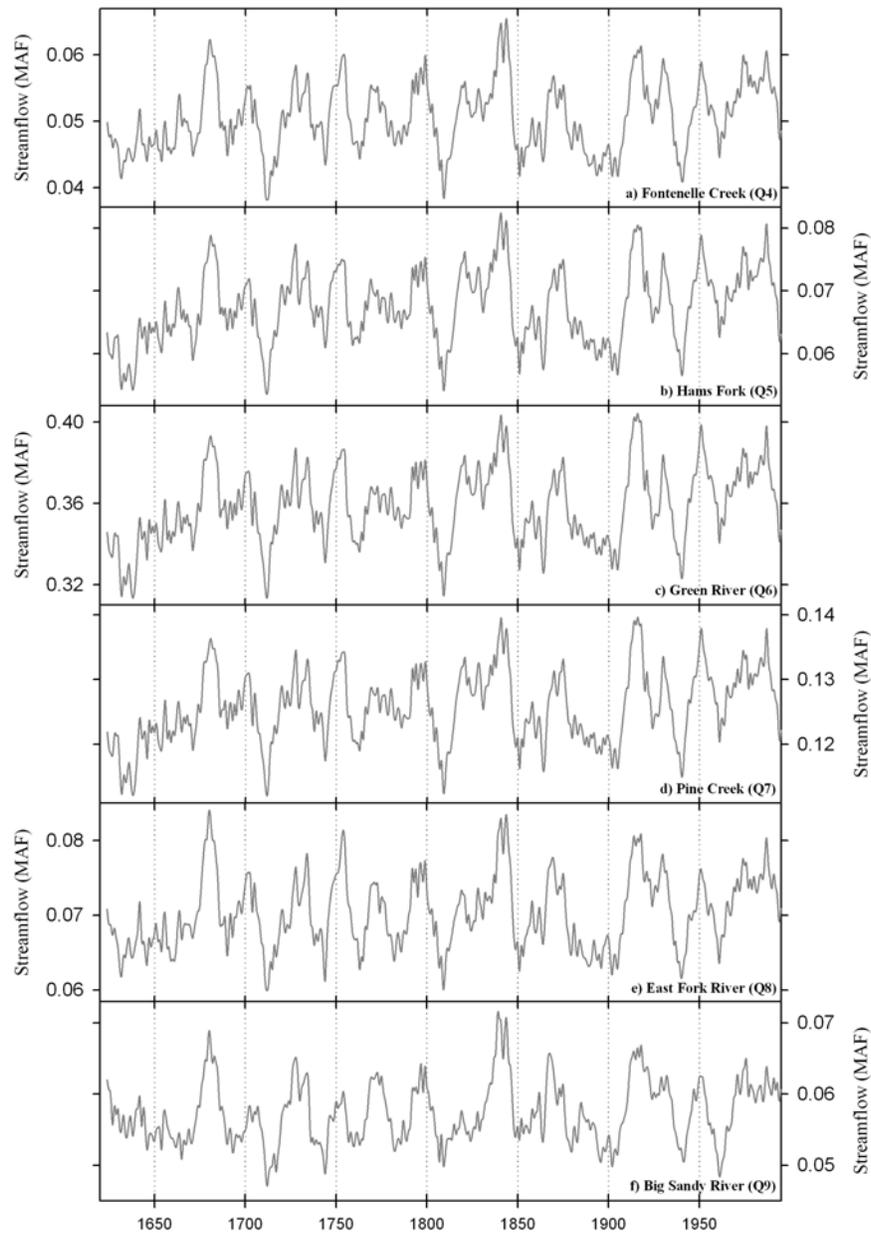
Figure 5: **Comparison of reconstructed streamflow for headwater stream gage stations with ten year filter (end year displayed) of water year discharge (excluding the Big Sandy River (Q9) where spring-summer discharge was reconstructed).**
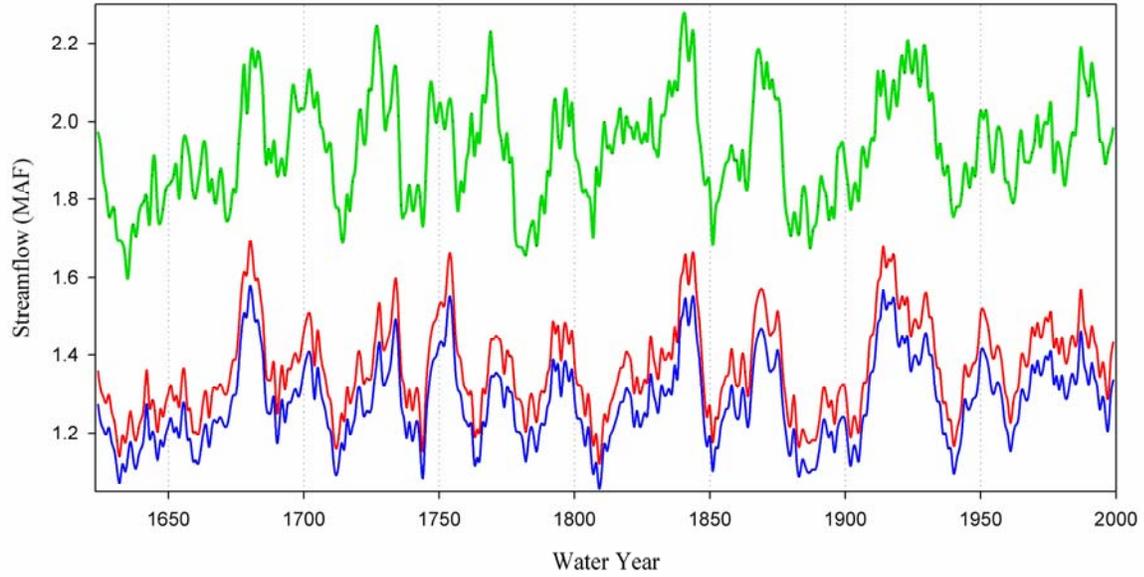
Figure 6: Comparison of reconstructed streamflow for CRSS nodes with a ten year filter (end year displayed); Green River near Greendale, UT (green line), Green River near Green River, WY (red line), and Green River below Fontenelle Reservoir, WY (blue line).
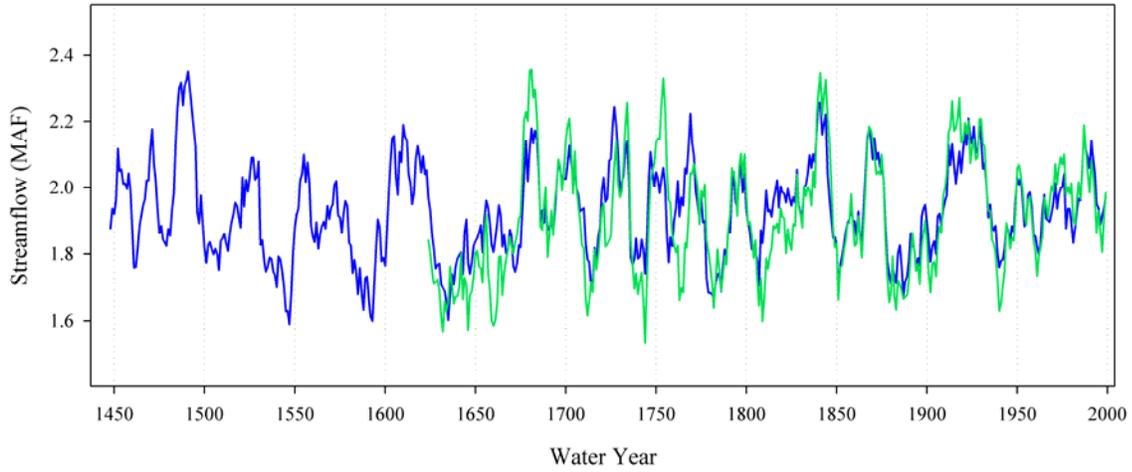
Figure 7: Comparison of the extended reconstruction (blue line) and the 1615-1999 reconstruction (green line), from 1615, the Green River near Greendale, UT. Data are plotted with a 10-year filter (end year displayed).
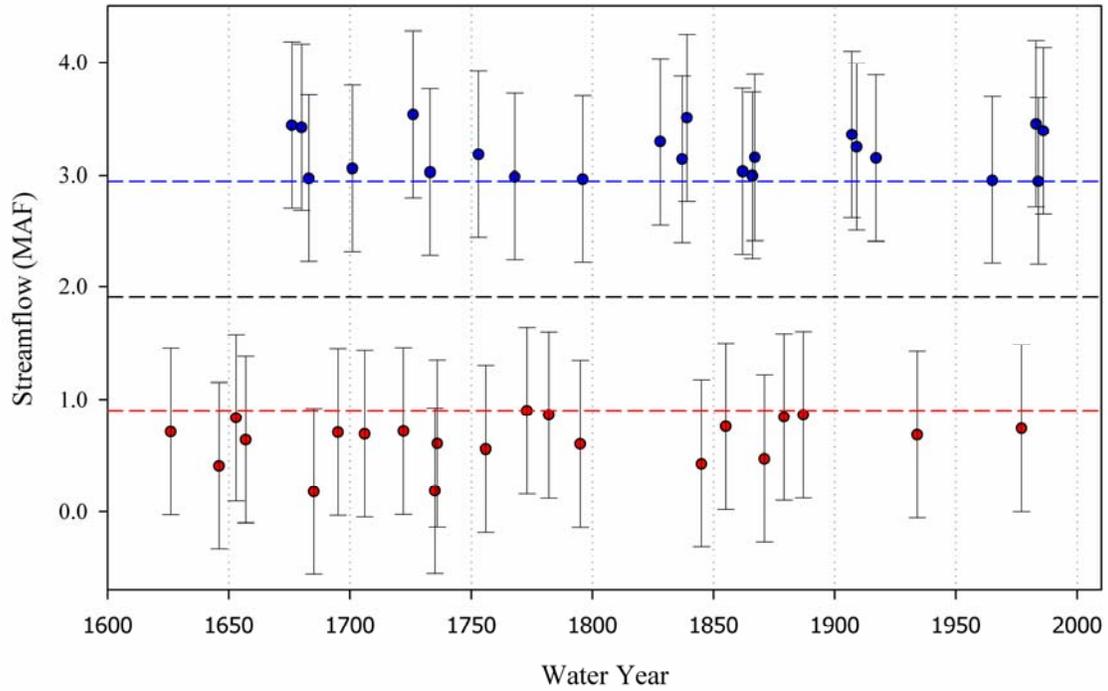
Figure 8: Significant wet years (blue dots) exceeding the 95th quantile (dashed blue line) and significant dry years (red dots) not exceeding the 5th quantile (dashed red line) for reconstructed Green River near Greendale, UT streamflow (1615-2004) plotted with the average flow of the reconstruction (dashed black line).
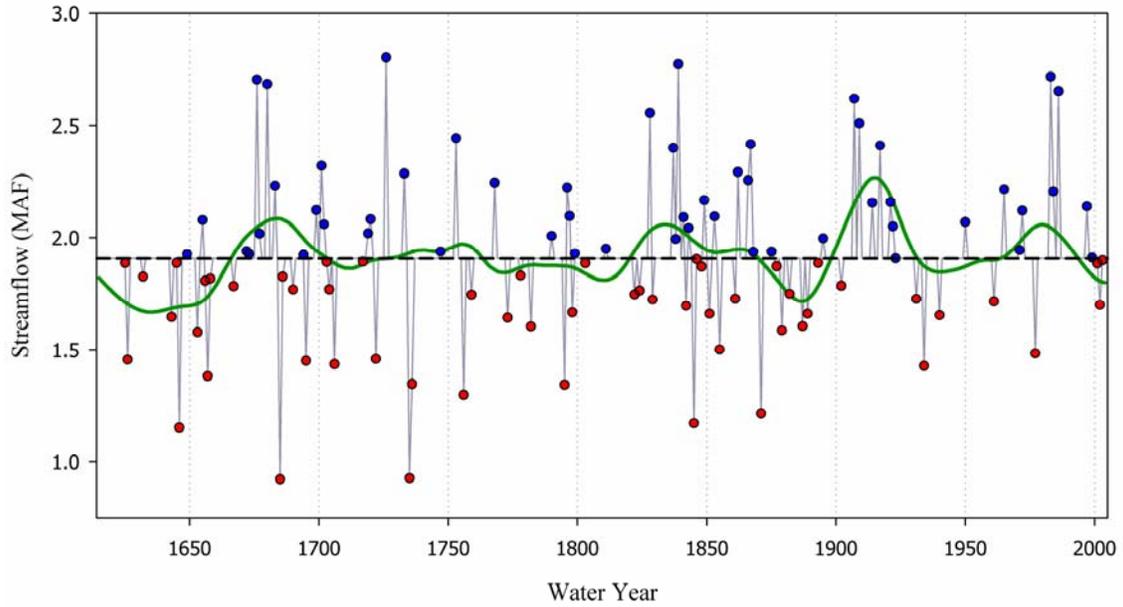
Figure 9: Significant wet years (blue dots) and significant dry years (red dots) for reconstructed Green River near Greendale, UT streamflow (1615-2004) plotted with the average flow of the reconstruction (dashed black line) and a 25 year cubic spline (green spline).
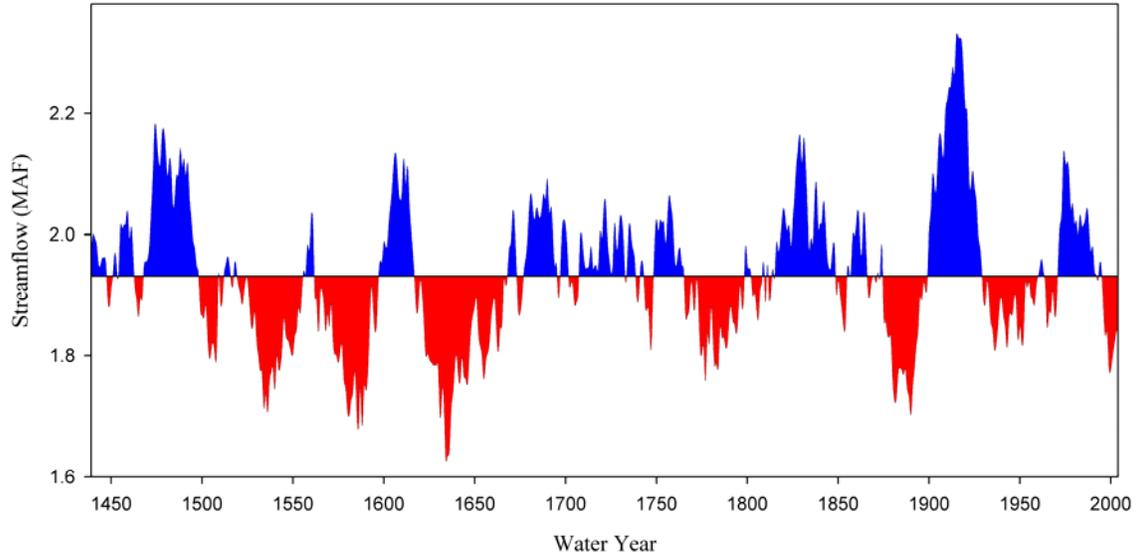
Figure 10: A 25-year moving average with deficit streamflow, based on the mean of the entire reconstructed record, (filled in red) and surplus streamflow (filled in blue), using an extended reconstruction (1439-2004) for the Green River near Greendale, UT.
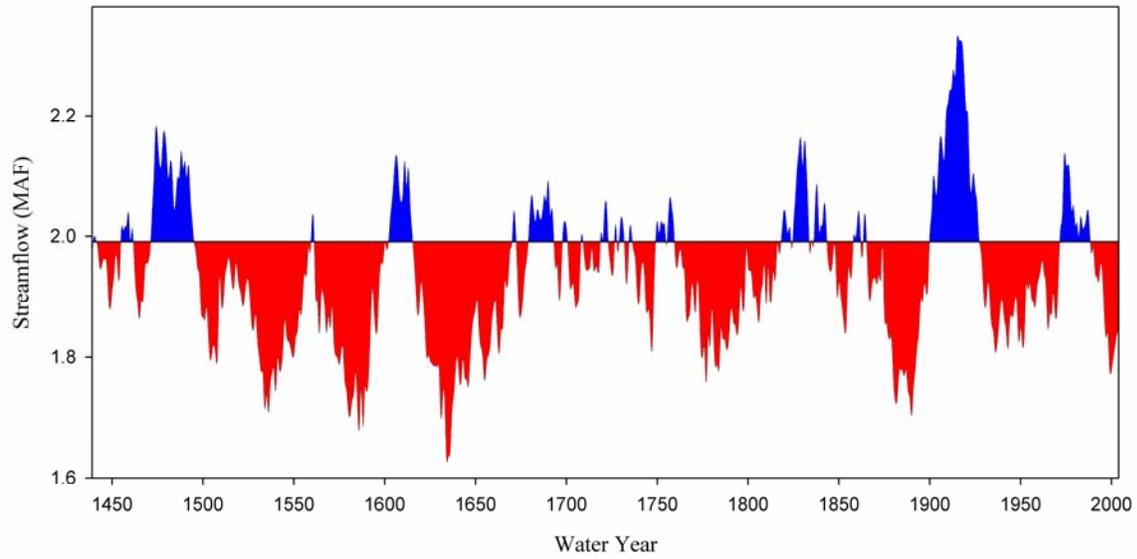
Figure 11: A 25-year moving average with deficit streamflow, based on the mean of the entire reconstructed record, (filled in red) and surplus streamflow (filled in blue), using an extended reconstruction (1439-2004) for the Green River near Greendale, UT.

Table 1: USGS stream gages selected for reconstruction.

ID[a]	Name	ID #	Gage Record	Basin Area (sq. miles)	r [e]
	USGS Stream Gage Information				
Q1	Green R. nr. Greendale, UT	09234500	1906-1995[c]	19350	0.23
Q2	Green R. nr. Green River, WY	09217000	1906-1995[c]	14000	0.19
Q3	Green R. bel. Fontenelle Res., WY	09211200	1906-1995[c]	4280	0.15
Q4	Fontenelle C. nr. Fontenelle, Wy[b]	09210500	1952-2006	152	0.07
Q5	Hams Fork nr. Frontier, Wy[b]	09223000	1953-2006	128	0.14
Q6	Green R. nr. Daniel, Wy[b]	09188500	1932-1992	468	0.04
Q7	Pine C. ab. Freemont Lake, WY	09196500	1955-1997	76	-0.06
Q8	East Fork R. nr. Big Sandy, WY	09203000	1939-1992	79	0.09
Q9	Big Sandy R. nr. Big Sandy, Wy[b]	09212500	1940-1987[d]	94	-0.06

[a]Gage identification shown on map in Figure 1.

[b]Full gage names – Fontenelle C. nr. Herschler Ranch, nr. Fontenelle, WY; Hams Fork below Pole Creek, nr. Frontier, WY; Green River at Warren Bridge, nr. Daniel, WY; Big Sandy R. at Leckie Ranch, nr. Big Sandy, WY.

[c]Record is naturalized flow (U.S.B.R.).

[d]Spring-summer instrumental record only.

[e]Significant autocorrelation (95% level).

Table 2: Descriptive statistics for new tree ring chronologies.

Site Name	Species	Elevation (feet)	Time Span (yr A.D.)	Year SSS > 0.85	Number of Trees	Number of Series	Inter-series Correlation
ARE	PIFL	8040-8440	1200-2006	1203	20	28	0.71
ARR	PSME	8530-8610	1519-2006	1615	25	53	0.77
BLE	PSME	7320-7500	1576-2006	1672	21	41	0.79
FMT	PSME	7500-8400	1507-2006	1603	35	70	0.77
FSE	PIFL	7650-8000	1654-2006	1692	23	35	0.80
RCU	PIFL	6500-6610	1600-2006	1613	24	41	0.69

Table 3: Correlation matrix of newly developed tree ring chronologies.

	ARE	ARR	BLE	FMT	FSE
ARR	0.74				
BLE	0.47	0.60			
FMT	0.54	0.63	0.80		
FSE	0.53	0.52	0.66	0.75	
RCU	0.45	0.45	0.32	0.32	0.32

Table 4: Reconstruction model calibration and verification statistics.

Gauge Name	Calibration Period	R^2	F	Mean[c]	RMSE[c]	CVSE[c]
Green River (Q1)	1914-1995	0.65	23.27[b]	1.909	0.370	0.403
Green River (Q1)[a]		0.50	19.21[b]	1.930	0.437	0.462
Green River (Q2)	1914-1995	0.60	28.43[b]	1.370	0.279	0.297
Green River (Q3)	1914-1995	0.59	27.29[b]	1.282	0.260	0.277
Fontentelle Creek (Q4)	1952-1999	0.48	14.09[b]	0.051	0.016	0.016
Hams Fork (Q5)	1953-1999	0.48	20.48[b]	0.069	0.022	0.022
Green River (Q6)	1932-1992	0.44	22.46[b]	0.358	0.062	0.064
Pine Creek (Q7)	1955-1997	0.53	22.73[b]	0.124	0.020	0.021
East Fork River (Q8)	1939-1987	0.58	22.81[b]	0.072	0.014	0.015
Big Sandy River (Q9)	1940-1987	0.54	12.52[b]	0.058	0.013	0.014

[a]Green River nr. Greendale, UT extended reconstruction.
[b]$p < 0.001$
[c]Mean, Root Mean Square Error (RMSE), and Cross Validated Standard Error (CVSE) are expressed in million acre-ft.

Table 5: Correlation matrix of reconstructed UGRB headwater stream gage stations.

	Q4	Q5	Q6	Q7	Q8
Q5	0.94				
Q6	0.90	0.96			
Q7	0.91	0.97	0.98		
Q8	0.93	0.85	0.87	0.87	
Q9	0.76	0.69	0.68	0.67	0.80

Table 6: Flow characteristic comparisons (in acre-ft) between instrumental and reconstructed water year records (not combined with instrumental gage record).

Variable	Instrumental Record				Reconstructed Record			
	Mean	StDev	Min	Max	Mean	StDev	Min	Max
Q1	1.992	0.642	0.659	3.495	1.909	0.552	0.392	3.343
Q2	1.421	0.455	0.440	2.569	1.370	0.360	0.401	2.345
Q3	1.329	0.418	0.454	2.453	1.282	0.329	0.397	2.173
Q4	0.051	0.021	0.018	0.112	0.051	0.016	0.009	0.104
Q5	0.069	0.031	0.013	0.155	0.069	0.022	0.008	0.127
Q6	0.364	0.081	0.203	0.556	0.358	0.058	0.184	0.500
Q7	0.128	0.029	0.070	0.183	0.124	0.023	0.056	0.180
Q8	0.074	0.022	0.031	0.129	0.072	0.018	0.025	0.121
Q9	0.059	0.018	0.025	0.105	0.058	0.014	0.009	0.105

Chapter 2 – Drought Frequency-Duration-Deficit Analysis

Abstract

The limited length of instrumental streamflow data impacts the true magnitude of natural interdecadal variability of water delivered from the UGRB. This limited period of instrumental record can be expanded by utilizing proxy records (reconstructed streamflow) derived from tree rings. Two reconstructed streamflow datasets are now available for the Green River near Green River, UT (Stockton and Jacoby, 1976; Woodhouse et al., 2006), and a new preliminary reconstruction has been developed for the Green River near Green River, Wyoming (Woodhouse et al., 2006). Also, recent research has resulted in the development of nine streamflow reconstructions spatially located throughout the UGRB (Barnett et al., 2008). The proposed research would use these streamflow reconstructions to assess patterns (temporal and spatial) and sources of streamflow variability in the UGRB. An investigation of long-term streamflow variability, focusing on extreme events such as mega-droughts, will be performed. The research will result in the development of probabilistic drought forecasts. Salas et al. (2005) provides drought definitions and equations that can be utilized by water planners in storage dependent systems. Loaiciga (2005) utilized the compound renewal process, which generalizes the Poisson process, to calculate return periods for drought events. This may result in frequency – duration curves for UGRB drought. Such probability curves can then be analyzed in light of Compact agreements to answer questions such as, "How often might the outflow from the UGRB fail to meet 10-year delivery obligations?"

Introduction

The Upper Green River Basin (UGRB, Figure 1) represents a vital water supply region for southwestern Wyoming and Upper / Lower Colorado River Compact states. Rapid development in the southwestern U.S. (e.g., Las Vegas, Phoenix) combined with the recent drought has greatly stressed the water supply system of the Colorado River. This has resulted in increased interest in the Colorado River Compact and related "Law of the River." The limited length of instrumental streamflow data impacts the true magnitude of natural interdecadal variability of water delivered from the UGRB. This limited period of instrumental record can be expanded by utilizing proxy records (reconstructed streamflow) derived from tree rings. Two reconstructed streamflow datasets are now available for the Green River near Green River, UT (Stockton and Jacoby, 1976; Woodhouse et al., 2006), and a new preliminary reconstruction has been developed for the Green River near Green River, Wyoming (Woodhouse et al., 2006). Also, recent research has resulted in the development of nine streamflow reconstructions spatially located throughout the UGRB (Barnett et al., 2008). Increasing the length of streamflow records will provide more accurate frequency and risk assessment of drought events. Water managers will be better able to plan for drought events and will have a better understanding of the true nature and variability in their river systems. Biondi et al., (2005) developed a stochastic model based on the theory of random sums to quantify droughts. Information provided from this model would include: (1) given a drought event (i.e., the recent 2000 to 2004 drought), there is an (X)% chance of a drought occurring of longer duration or magnitude; (2) a drought of such magnitude has a (Y)% chance of lasting for (Z) years or longer. This type of question can also be answered by the drought definitions and analysis presented by Salas et al. (2005). The inherent scarcity of water in the semiarid to arid regions of the southwestern United States is exacerbated by the occurrence of frequent and persistent droughts (Stockton et al., 1991; Tarboton, 1994). Drought events can

be defined in many ways and each definition will change as analysis needs change. Meko et al. (1995) cites Sastri et al. (1982) as reporting that there were more than 60 definitions of drought found in literature. Young (1995) provides two possible definitions of drought based in meteorological terms, limited or no rainfall, or agricultural terms, available soil moisture for evapotranspiration. Young (1995) selected a hydrologic measure as a drought indicator that follows the same parameters as Tarboton (1994). This research utilizes the drought definition presented by Tarboton (1994) and his referenced authors: A drought is defined as a consecutive series of years during which the average annual streamflow is continuously below some specified threshold level, which is typically taken to be the long-term mean (Tarboton, 1994). The most recent identified drought generally lasted from 2000 to 2004, although differing analysis methods may reduce this window or have no drought identified. This drought is used as a defining or threshold event.

Data
Four streamflow reconstructions from Barnett et al. (2008) were used for drought analysis in the UGRB. The four stream flow gages are denoted as Q1, Q3, Q5, and Q7 (Table 1, Figure 1). United States Geological Survey (USGS) stream gage information was obtained for all stream gages in the UGRB from the National Water Information System (NWIS) (http://waterdata.usgs.gov/nwis/sw). Few gages in the UGRB have a continuous 40-50 year instrumental record necessary to calibrate a regression model while remaining unimpaired. Unimpaired stations were identified using the Hydro-Climatic Data Network (HCDN) (Barnett et al., 2008; Slack et al., 1993; Wallis et al., 1991). Stream gages with naturalized data were provided by the United States Bureau of Reclamation (USBR) (Barnett et al., 2008; Prairie, 2004) at river nodes used in the Colorado River Simulation System (CRSS) (Barnett et al., 2008). Gage records for Q1 and Q3 are naturalized records while records for Q5 and Q7 are unimpaired. Naturalized or unimpaired records provide streamflow data that would occur absent anthropogenic interference. Barnett et al. (2008) utilized tree ring chronologies to create reconstructed records that were integrated with gage records to produce the final water year records used in this paper (Figure 2). The final reconstructed records were rescaled to force the standard deviation in the reconstruction to be equal to that of the stream gage record (Barnett et al., 2008; Timilsena et al., 2007).

Methodology

A drought occurs when an individual reconstructed water year's value (x_i) is below a defined threshold creating a deficit (d_i). The threshold used in this part of the study is the mean (μ) of the entire reconstructed record (1615-2004). The duration (L_i) of a drought event is the sum of consecutive years with values, or running averages, below the mean ($x_i < \mu$). The beginning year of a drought is the year when $x_i < \mu$ and the end year is the last consecutive year below the threshold. The magnitude (M_i) of a drought is the sum of all deficits included in the duration. The severity (S_i) of a drought is obtained by dividing magnitude by duration (M_i / L_i).

Drought Magnitude (Method 1)
The first analysis technique (Method 1) used to identify and compare drought events follows those used by Timilsena et al. (2007). Method 1 consists of 5 parts denoted Method 1a through

Method 1e. Method 1a only considers droughts with duration of 2 years or more. As stated by Timilsena et al. (2007), this method does not take long periods of drought into account because a single x_t value equal to or above the threshold (creating a surplus) causes the duration to end. Longer dry periods with multi-year averages below the threshold are analyzed by taking moving averages of the entire record. Moving averages of 3, 5, 7, and 10 years (Figure 3) are offset at the beginning of the reconstructed record to include the end year of 2004. These methods are denoted 1b, 1c, 1d, and 1e respectively. When drought events are sorted according to magnitude (deficit: absolute value of magnitude), the probability (ρ) and return period (R) can be determined by a Weibull distribution (Equation 1, Equation 2).

$$\rho = \frac{m}{(N+1)} \tag{1}$$

$$R = \frac{1}{\rho} \tag{2}$$

$$N = \Sigma \text{ (all recorded events)} = 390 \tag{3}$$

Where: m is the rank of an event, the largest drought in deficit or intensity is ranked 1, and R is in years.

Drought Severity (Method 2)

The second analysis technique (Method 2) uses a compound renewal approach (Timilsena et al., 2007; Loaiciga, 2005). Method 2 considers an event's magnitude as well as its duration. This is accomplished by only considering drought events that are equal to or greater than a defined event or threshold (θ). The defining event for this research is the most recent drought (~2000-2004). The only events considered are equal to or greater than $L_{current}$ ($\theta = 5$; i.e., length of recent drought) and $M_{current}$ simultaneously. The renewal time ($\bar{R}$) is equal to the sum of the expected values duration (L) and interval time (T) or:

$$\bar{R} = \theta + \frac{1}{a_1} + \frac{1}{a_2} \tag{4}$$

$$a_1 = \frac{1}{(L - \theta)} \tag{5}$$

$$a_2 = \frac{1}{T} \tag{6}$$

The parameters a_1 and a_2 are representative of the average duration ($\bar{L}$) and average interval time ($\bar{T}$) between selected events. Equation 4 assumes that $a_1 \neq a_2$. The time before the first selected event and the time after the last selected event are not considered in the average interval time.

Drought Risk (Method 3)

The third analysis technique (Method 3) characterizes droughts by defining four drought events, $P(E)$, to analyze severity and risk (Salas et al., 2005). Case 1 events (Equation 7) are characterized by droughts with accumulated deficit (D) greater than a specified deficit (D_0) and duration (L) equal to an analyzed event's duration or threshold duration (l_0). Case 1 droughts

can be analyzed for duration only, by setting the specified deficit to zero ($D_0 = 0$). Case 2 events (Equation 8) are similar to Case 1, however the duration is greater than or equal to the threshold duration ($L \geq l_0$). Events can be analyzed without regard for duration by setting $L \geq 1$ and regardless of deficit by setting $D > 0$. Cases 3 and 4 (Equations 9 and 10 respectively) utilize the same analytical procedures as Cases 1 and 2 by replacing deficit with intensity ($I = L/D$). The occurrence probability of each case is described by the bivariate probability distribution functions (pdfs) shown in equations 7 through 10. Each expression follows a gamma distribution characterized by their individual shape (r) and scale (β) factors. The shape and scale factors used in the equations were obtained by plotting all identified droughts, for each Method 1 scenario, with a gamma distribution. Each expression is also defined by a prescribed length (l_0) and deficit (D_0) or intensity (I_0), where intensity is the same as severity as defined above. Transition probabilities (p_{xx}) can be calculated for each water year record with equations 11 and 12 (Jackson, 1975 and Fernández et al., 1999). It is assumed that the sequence of surpluses (denoted by 1) and deficits (denoted by 0) follow a Markov chain. The number of transitions (N) from fail (f) to safe (s) or 0 to 1 is the number of times that the water year record transitions from a drought event to a surplus event. This process is also used for transitions from safe to fail, fail to fail, and safe to safe. The return period (T) of any event described by Salas et al. (2005) can be evaluated with Equation 13.

$$P[D > D_0, L = l_0] = \int_{D_0}^{\infty} \frac{1}{\beta \Gamma(l_0 r)} \left(\frac{z}{\beta}\right)^{l_0 r - 1} e^{-z/\beta} p_{01} (1 - p_{01})^{l_0 - 1} dz \tag{7}$$

$$P[D > D_0, L \geq l_0] = \int_{D_0}^{\infty} \sum_{i=l_0}^{\infty} \frac{1}{\beta \Gamma(ir)} \left(\frac{z}{\beta}\right)^{ir - 1} e^{-z/\beta} p_{01} (1 - p_{01})^{i-1} dz \tag{8}$$

$$P[I > I_0, L = l_0] = \int_{I_0}^{\infty} \frac{1}{\beta \Gamma(l_0 r)} \left(\frac{l_0 z}{\beta}\right)^{l_0 r - 1} e^{-l_0 z/\beta} p_{01} (1 - p_{01})^{l_0 - 1} dz \tag{9}$$

$$P[I > I_0, L \geq l_0] = \int_{I_0}^{\infty} \sum_{i=l_0}^{\infty} \frac{1}{\beta \Gamma(ir)} \left(\frac{iz}{\beta}\right)^{ir - 1} e^{-iz/\beta} p_{01} (1 - p_{01})^{i-1} dz \tag{10}$$

$$p_{fs} = p_{01} = \frac{N_{fs}}{N_{ff} + N_{fs}} \tag{11}$$

$$p_{sf} = p_{10} = \frac{N_{sf}}{N_{ss} + N_{sf}} \tag{12}$$

$$T = \frac{p_{01} + p_{10}}{p_{01} p_{10}} \frac{1}{P(E)} \tag{13}$$

Results
Rankings for Method 1a through 1e are summarized in Tables 2 and 3. Table 2 shows identified drought ranks when sorted for magnitude. Table 3 shows identified drought ranks when sorted for severity. The recent drought rank is reported for each ranking method along with the top five drought events. Return periods for Method 1 and 2 are reported on the left hand side of Table 2. As seen in Figure 2 and Table 2, the deficit created by the most recent drought (~2000-2004) is a notable event but it is not the greatest event of record. If gage station Q1 is considered, the ranking and return times for Methods 1 and 2 diminishes as longer moving averages are considered. This shows that the years leading up to that event were, on average, in surplus. This trend is not the same when gage station Q1 is considered for severity, Table 3. The recent drought event is ranked 2nd and 1st for the 3 and 5 year moving averages (Method 1b and 1c

respectively), while ranked 5th for when droughts of a minimum 2 year duration are considered (Method 1a). This shows that the recent event does not exhibit the greatest deficit for drought events, however its severity is the greatest when examining a 3 to 5 end-year average. Figure 4 illustrates the solutions for Method 3 Case 1 (Equation 7) when only duration is considered ($D_v = 0$). The solutions for each gage station are plotted together with Q5 and Q7 overlapping one another. As seen in Figure 4, the return period for a 5 year duration drought is roughly 100 years. This method also allows the estimation of greater return periods as compared to Method 1 & 2. When Equation 7 is used to evaluate the recent drought, Method 1a ($D > 3653818, L = 5$), the return period is 133 years. Graphical solutions for Equation 7 are shown in Figure 5.

Conclusions
The use of dendrochronology to create reconstructed streamflow records can improve stochastic estimates of streamflow variations by extending the available period of record. The reconstructed period of record contains drought events that well surpass any events that would be part of the instrumental record, in terms of magnitude and duration. The mean for instrumental and reconstructed records are of notable difference (Table 1). This is caused by the wet period in the early 20th century exemplified in the instrumental record and the long dry period exemplified in the early 17th century (Figure 3). Methods 1 and 2 are directly dependent on the reconstructed record for the calculation of return periods. This dependence creates scaling errors in return period. Method 1 return periods are limited to bin sizes that are dependent on the record length. The difference between return periods becomes more pronounced at the less probable values. As in this paper, the largest possible return period for Method 1 is 391 years. Method 2 is similarly limited to return periods based on the number of observed events and the time between. Method 3 is based on the same record, however it allows for the interpolation of greater return periods than Methods 1 and 2. Future research may focus on identifying climate drivers (e.g., ENSO) of UGRB drought events.

References

Barnett, F. A., S. Watson, S. Gray, G. Tootle, 2008, Upper Green River Basin streamflow reconstructions and drought analysis (in preparation).

Biondi, F., T. J. Kozubowski, A. K. Panorska (2005), A new model for quantifying climate episodes, *Int. J. Climatol.*, 25: 1253-1264, doi:10.1002/joc.1186.

Fernández, B., J. D. Salas (1999), Return period and risk of hydrologic events. I: Mathematical formulation, J. *Hydrologic Eng.*, 4(4), 297-307.

Jackson, B. B. (1975), Markov mixture models for drought lengths, *Water Resour. Res.*, 11(1), 64-74.

Loáiciga, H. A. (2005), On the probability of droughts: The compound renewal model, *Water Resour. Res.*, 41, W01009, doi:10.1029/2004WR003075.

Meko, D., C. W. Stockton, W. R. Boggess (1995), The tree-ring record of severe sustained drought, *Water Resour. Bull.*, 31(5), 789-801.

Prairie, J. (2004), Naturalized flows 1906-2004 for the Colorado River Basin, U.S. Bureau of Reclamation.

Salas, J. D., C. Fu, A. Cancelliere, D. Dustin, D. Bode, A. Pineda, E. Vincent (2005), Characterizing the severity and risk of drought in the Poudre River, Colorado,

Journal of Water Resources Planning and Management, doi:10.1061/(ASCE)0733
9496(2005)131:5(383).

Sastri, A. S. R. A. S., Y. S. Rama Krishna, B. V. Ramana Rao (1982), Droughts in
western Rajahsthan. Divisional technical report 1-82, Division of wind power and solar
energy utilization, Central Arid Zone Research Institute, Jodhpur- 342 003.

Slack, J. R., A. Lumb, J. M. Landwehr (1993), Hydro-Climate Data Network (HCDN)
Streamflow Data Set, 1874-1998. CD-ROM. U.S. Geologica Survey, Reston, Virginia,
U.S.A. Available from Oak Ridge National Laboratory Distributed Active Archive
Center, Oak Ridge, Tennessee, U.S.A. [http://www.daac.ornl.gov].

Stockton, C.W., and G.C. Jacoby (1976), Long-term surface water supply and streamflow trends
in the Upper Colorado River Basin, *Lake Powell Research Project Bulletin* No. 18,
National Science Foundation, Arlington, VA.

Stockton, C. W., D. Meko, W.R. Boggess (1991), Drought history and reconstructions from tree
rings. In: Severe sustained drought in the southwestern United States, Phase 1 Report to
the US Department of State, Man and Biosphere Program, Ch. 1.

Tarboton, D. G. (1994), The source hydrology of severe sustained drought in the
southwestern United States, *Journal of Hydrology*, 161:31-69.

Timilsena, J., T. C. Piechota, H. Hidalgo, G. Tootle (2007), Five hundred years of
hydrological drought in the Upper Colorado River Basin, *Journal of the
American Water Resources Association* (JAWRA), 43(3): 798-812, doi:10.1111/j.1752
1688.2007.00064.x

Wallis, J.R., D. P. Lettenmaier, E. F. Wood (1991), A daily hydro-climatical data set for the
continental United States, *Water Resources Research*, 27(7), 1657- 1663.

Woodhouse, C. A., S. T. Gray, D. M. Meko (2006), Updated streamflow reconstructions for the
Upper Colorado River Basin, *Water Resour. Res.*, 42, W05415,
doi:10.1029/2005WR004455.

Young, R. A. (1995), Coping with a severe sustained drought in the Colorado River:
Introduction and Overview, *Water Resour. Bull.*, 31(5), 779-788.
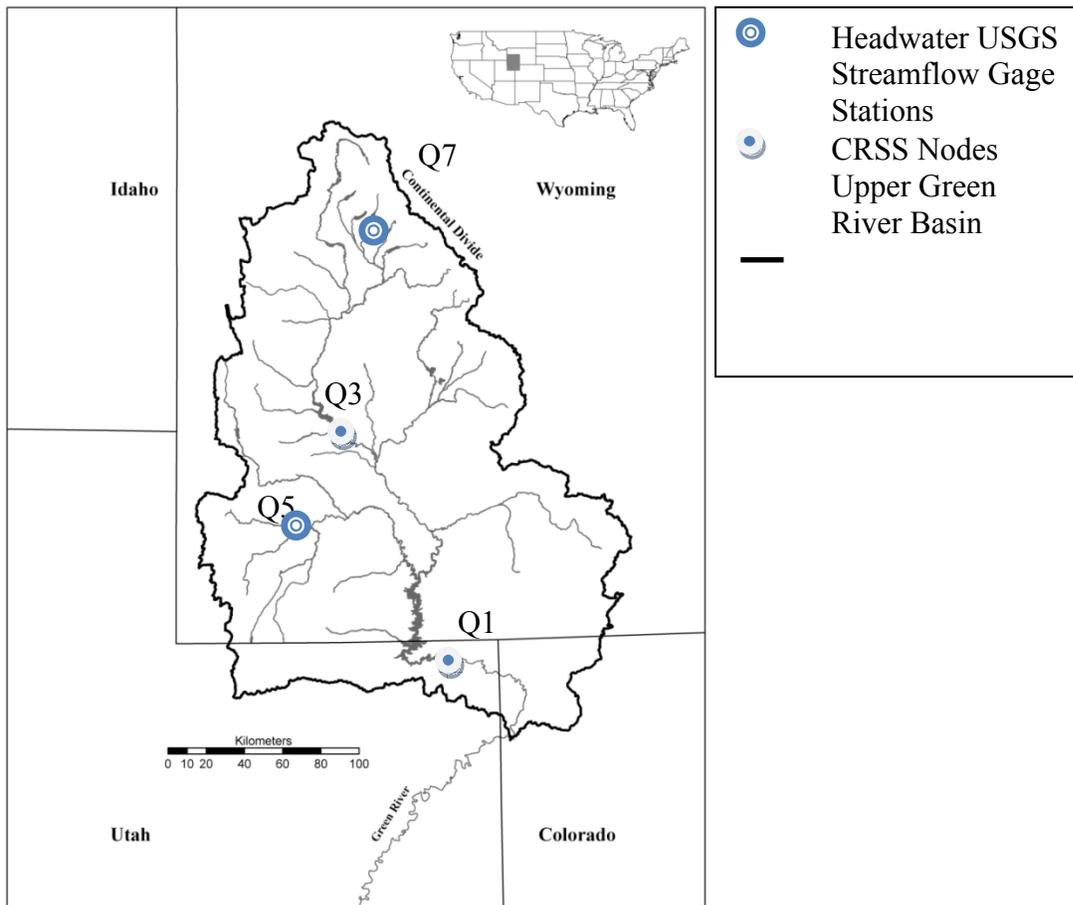
Figure 1: Upper Green River Basin
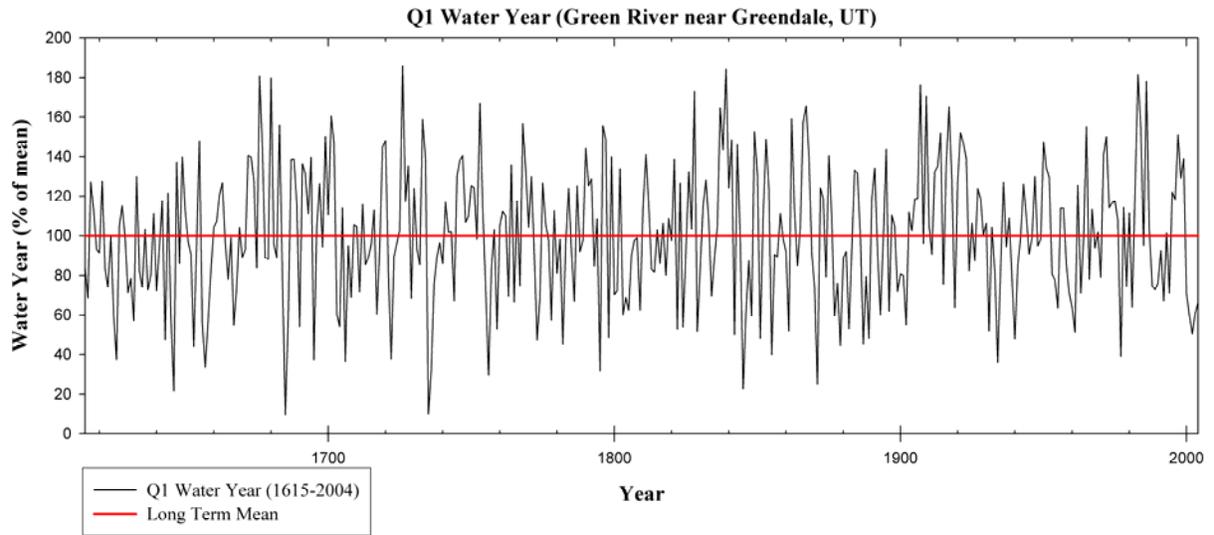
Figure 2: Q1, Reconstructed Water Year (1615-2004)
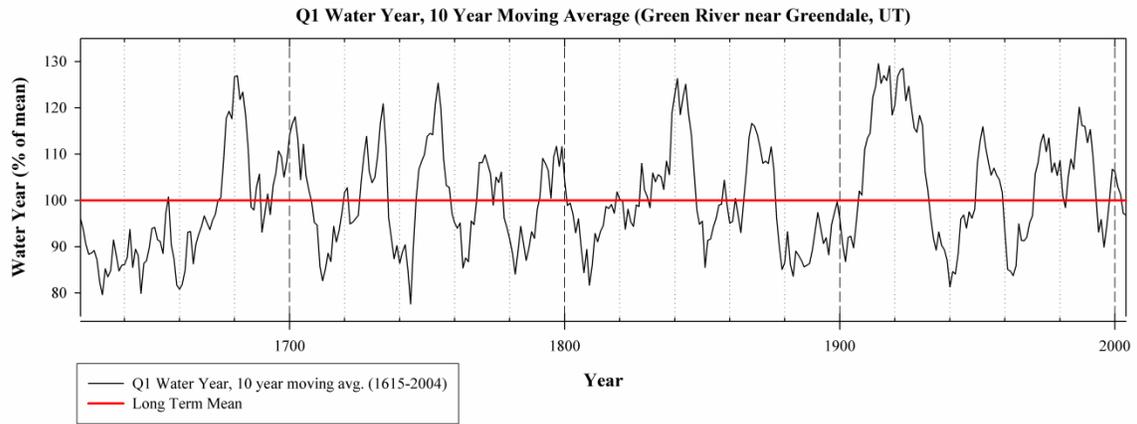
Figure 3: Q1, 10 Year Moving Average (1624-2004)
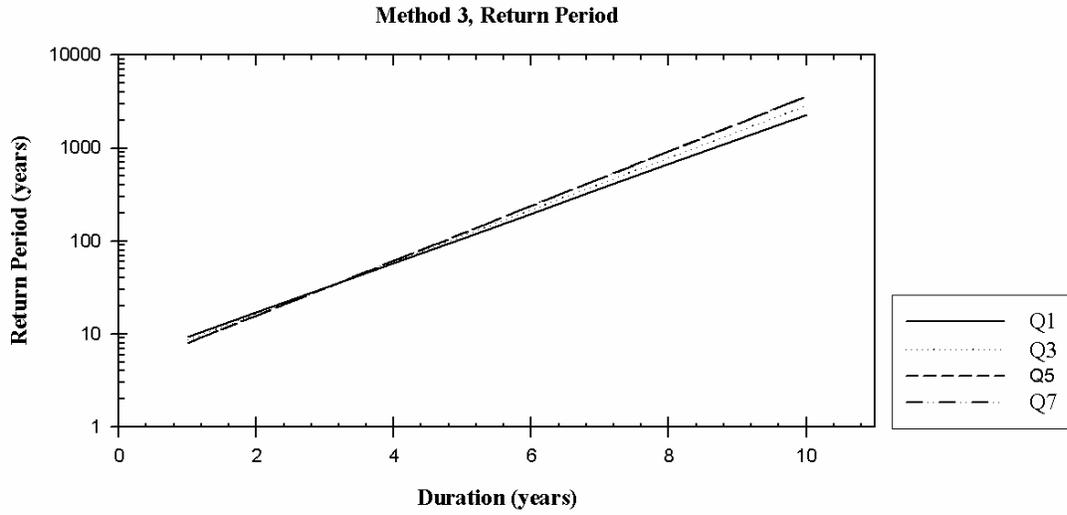
Figure 4: Method 3, Return Periods for Duration Only
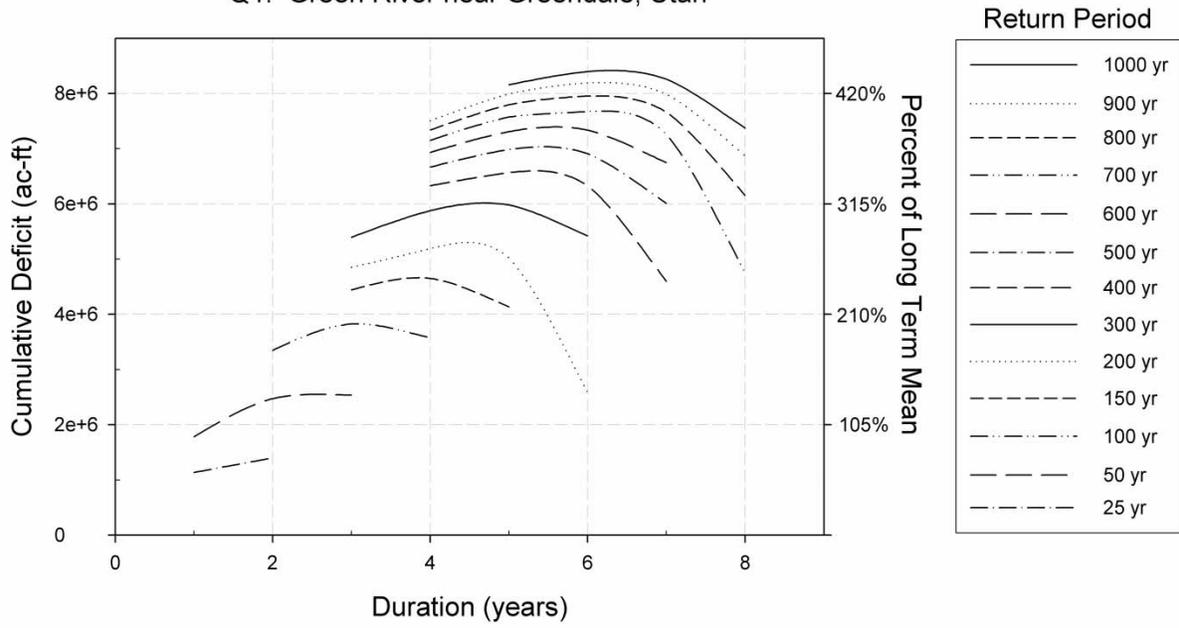
Figure 5: Frequency, Duration and Deficit Curves

Table 1: USGS Stream Gage Information and Reconstructed Mean

					Basin Area	Reconstructed Mean	Instrumental Mean
	USGS Stream Gage Information						
ID[a]	Name	ID #	Gage	Record	(sq. kilometers)	(m^3)	(m^3)
Q1	Green R. nr. Greendale, UT	9234500		1906-1995[c]	50116	2.35E+09	2.46E+09
Q3	Green R. bel. Fontenelle Res., WY	9211200		1906-1995[c]	11085	1.57E+09	1.64E+09
Q5	Hams Fork nr. Frontier, Wy[b]	9223000		1953-2006	332	8.44E+07	8.49E+07
Q7	Pine C. ab. Freemont Lake, WY	9196500		1955-1997	197	1.53E+08	1.58E+08

[a]Gage identification shown on map in Figure 1.

[b]Full gage name: Hams Fork below Pole Creek, nr. Frontier, WY

[c]Record is naturalized flow (U.S.B.R.)

Table 2: Ranking Sorted for Magnitude

Gage Station	Drought Identificaiton Method 1	Ranked 1st	Ranked 2nd	Ranked 3rd	Ranked 4th	Ranked 5th	Rank of Recent Drought	Average Duration (years)
	a	1735-1740	1877-1883	2000-2004	1844-1848	1656-1659	# 3 (2000-2004)	3
	b	1630-1648	1704-1719	1653-1661	1878-1884	1736-1742	# 8 (2001-2004)	4
Q1	c	1623-1650	1932-1944	1653-1662	1706-1718	1735-1742	# 17 (2002-2004)	6
	d	1624-1652	1879-1895	1931-1946	1656-1664	1706-1719	# 19 (2003-2004)	7
	e	1624-1655	1877-1906	1657-1673	1933-1949	1801-1818	# 18 (2003-2004)	9
	a	1877-1883	1844-1848	1803-1809	2000-2004	1735-1740	# 4 (2000-2004)	3
	b	1800-1810	1878-1884	1704-1715	1844-1849	1653-1660	# 8 (2001-2004)	4
Q3	c	1878-1894	1622-1641	1931-1944	1801-1811	1845-1852	# 16 (2002-2004)	6
	d	1879-1906	1624-1651	1931-1946	1803-1813	1706-1719	# 16 (2003-2004)	7
	e	1624-1673	1877-1908	1933-1949	1801-1816	1708-1719	# 15 (2003-2004)	10
	a	1703-1711	1803-1809	2000-2004	1844-1848	1931-1936	# 3 (2000-2004)	3
	b	1704-1713	1630-1639	1802-1810	1989-1996	1896-1906	# 8 (2001-2004)	4
Q5	c	1619-1640	1704-1715	1804-1811	1896-1906	1933-1941	# 12 (2001-2004)	5
	d	1879-1907	1621-1641	1704-1718	1803-1813	1934-1942	# 14 (2002-2004)	6
	e	1624-1655	1878-1908	1706-1718	1804-1815	1993-2004	# 5 (1993-2004)	8
	a	1703-1711	1803-1809	1629-1632	1931-1936	1844-1848	# 20 (2000-2004)	3
	b	1630-1639	1704-1713	1802-1810	1932-1938	1897-1904	# 19 (2001-2004)	4
Q7	c	1619-1641	1887-1906	1704-1713	1804-1811	1933-1941	# 19 (2002-2004)	6
	d	1621-1643	1880-1907	1803-1813	1706-1715	1934-1941	# 20 (2004)	6
	e	1624-1655	1878-1908	1802-1815	1706-1718	1935-1943	No Drought	7

Table 3: Ranking Sorted for Severity

Gage Station	Drought Identification Method 1	Ranked 1st	Ranked 2nd	Ranked 3rd	Ranked 4th	Ranked 5th	Rank of Recent Drought	Number of Identified Droughts
Q1	a	1645-1646	1684-1686	1656-1659	1703-1704	2000-2004	# 5 (2000-2004)	51
	b	1685-1687	2001-2004	1736-1741	1871-1873	1887-1890	# 2 (2001-2004)	47
	c	2002-2004	1878-1884	1735-1742	1653-1662	1667-1671	# 1 (2002-2004)	35
	d	1656-1664	1803-1811	1846-1852	1624-1652	1735-1745	# 7 (2003-2004)	29
	e	1736-1745	1624-1655	1657-1673	1960-1970	1877-1906	# 19 (2003-2004)	23
Q3	a	1703-1704	1625-1626	1645-1646	1684-1686	1844-1848	# 7 (2000-2004)	50
	b	2001-2001	1878-1884	1685-1687	1844-1849	1736-1740	# 1 (2001-2004)	52
	c	2002-2004	1845-1852	1645-1661	1801-1811	1991-1996	# 1 (2002-2004)	37
	d	1846-1852	1656-1663	1803-1813	1992-1996	1879-1906	# 6 (2003-2004)	31
	e	1877-1908	1801-1816	1933-1949	1708-1719	1624-1673	# 15 (2003-2004)	21
Q5	a	1919-1920	1684-1686	1901-1902	1625-1626	1886-1887	# 8 (2000-2004)	42
	b	2001-2004	1846-1849	1685-1687	1704-1713	1802-1810	# 1 (2001-2004)	53
	c	1804-1811	2001-2004	1845-1852	1989-1996	1756-1761	# 2 (2001-2004)	40
	d	1846-1853	1803-1813	1621-1641	2002-2004	1934-1942	# 4 (2002-2004)	32
	e	1804-1815	1706-1718	1624-1655	1936-1943	1878-1908	# 6 (1993-2004)	26
Q7	a	1919-1920	1625-1626	1684-1686	1629-1632	1721-1722	# 37 (2000-2004)	45
	b	1846-1849	1685-1687	1630-1639	1704-1713	1802-1810	# 17 (2001-2004)	48
	c	1804-1811	1704-1713	1933-1941	1845-1852	1619-1641	# 12 (2002-2004)	36
	d	1706-1715	1934-1941	1803-1813	1846-1853	1621-1643	# 16 (2004)	35
	e	1624-1655	1706-1718	1802-1815	1935-1943	1878-1908	No Drought	29

Chapter 3 – Oceanic Atmospheric Variability and Drought

Abstract
A study of the influence of interdecadal and interannual Pacific oceanic / atmospheric variability on the Wind River Range (WRR), Wyoming is presented. The WRR is an unbroken 160-kilometer barrier that is host to 63 glaciers, the largest concentration of glaciers in the American Rocky Mountains. Glacial recession over the past half century has resulted in an increased interest in the region. Instrumental datasets were obtained for unimpaired streamflow and snow water equivalent for stations in the Green River Basin (GRB – west slope of WRR) and the Wind-Bighorn River Basin (WBRB – east slope of WRR). The phases (cold or warm) of Pacific [El Niño-Southern Oscillation (ENSO) and Pacific Decadal Oscillation (PDO)] oceanic / atmospheric phenomena were identified. Statistical significance testing of the datasets, based on the interdecadal and interannual oceanic / atmospheric phase (warm or cold), was performed applying the parametric t-test test. The results show that the interannual ENSO phase influences streamflow and snow variability in the WRR and the interdecadal PDO phase influences snow variability during La Niña events.

Introduction
The Wind River Range (WRR) is located in western-central Wyoming and is the headwaters of the Green River (tributary to the Colorado River) and the Wind River (tributary of the Missouri and Mississippi Rivers). The WRR is an unbroken 160-kilometer barrier that is host to 63 glaciers, the largest concentration of glaciers in the American Rocky Mountains (Figure 1).

As with many mountain glaciers in the Northern Hemisphere, the recession of Dinwoody Glacier (Figure 1) has been documented on a number of occasions since the mid-1800's (Wolken, 2000). The prominent recession of Dinwoody Glacier was noted in the 1930's. The 1940's and 1950's were a period of a slower rate of recession, with the estimated surface area of Dinwoody Glacier at 3.47 km^2 (Meier and Post 1962). A period of accelerated rate of recession followed, with the next quantitative evaluation estimating Dinwoody Glacier's surface area at 2.90 km^2 in the late 1980's (Pochop, et al. 1989). The most recent mapping of the surface area and elevation of Dinwoody Glacier was in 1999, where the surface area was estimated as only 2.33 km^2 (Wolken, 2000).

There is an increasing awareness that the oceanic / atmospheric variability occurs on interannual and interdecadal time scales. Furthermore, recent studies have shown the influence of coupled oceanic / atmospheric variability on climate of regions around the world. The study presented here investigates WRR hydrologic response to the influences of the El Niño-Southern Oscillation (ENSO) and the Pacific Decadal Oscillation (PDO).

ENSO refers to the interaction of the periodic large-scale warming or cooling of the central-eastern equatorial Pacific Ocean with the Southern Oscillation, a large-scale atmospheric pressure pattern across the tropical Pacific. The warm phase of ENSO is referred to as El Niño and the cool phase is referred to as La Niña. ENSO displays a periodicity of two (2) to seven (7) years (Philander, 1990). The PDO is a oceanic / atmospheric phenomena associated with persistent, bimodal climate patterns in the northern Pacific Ocean (poleward of 20° north) that oscillate with a characteristic period on the order of 50 years (a particular phase of the PDO will typically persist for about 25 years) (Mantua, et al., 1997).

Recent research has focused on the coupling of the interannual ENSO phenomenon with the PDO. Gershunov and Barnett (1998) evaluated the PDO's influence on ENSO for sea level pressures and heavy daily precipitation in the Atlantic / Pacific Oceans and continental United States. El Niño (La Niña) signals were found to be strong and stable during the warm (cold) PDO phase. Harshburger et al. (2002) determined that the largest departures for Idaho spring streamflow occurred during the La Niña / PDO cold phase. This is consistent with the findings of Gershunov and Barnett (1998) that ENSO (El Niño or La Niña) is strongest during the similar PDO (warm or cold) phase. In forecasting Columbia River streamflow, Hamlet and Lettenmaier (1999) defined six climate categories for ENSO (warm, cold or neutral) and PDO (warm or cold). The utilization of the climate categories significantly improved long lead-time forecasts. Also in the Pacific Northwest, Beebee and Manga (2004) found significant relationships between seasonal streamflow and, both ENSO and PDO. Hidalgo and Dracup (2001 and 2003) evaluated spring-summer streamflow and rainfall in the Upper Colorado River basin, considering the influence of ENSO and PDO and acknowledged a possible ENSO – PDO modulation of cold season precipitation.

The goal of the research presented here is to evaluate GRB / WBRB hydrology as influenced by interdecadal and interannual Pacific oceanic / atmospheric variability. In determining areas influenced by atmospheric / oceanic variability, verification was accomplished by parametric statistical testing.

Data
The major datasets used to develop the relationships between Pacific oceanic / atmospheric variability and hydrologic variability are instrumental unimpaired streamflow and snowfall data for the GRB and WBRB, and, oceanic / atmospheric data for the Pacific Ocean.

Unimpaired streamflow stations in the GRB and WBRB were identified from Wallis et al. (1991) (Figure 2 and Table 1). Monthly streamflow data was obtained from the U.S. Geological Survey (USGS) NWISWeb Data retrieval (http://waterdata.usgs.gov /nwis/). The average monthly streamflow rates (in cubic feet per second – cfs) were averaged for the water-year (October of the previous year to September of the current year) and converted into streamflow volumes (km^3) with proper conversions. The period of record for the streamflow data varied from station to station. The Natural Resources Conservation Service (NRCS) maintains a remote-sensing system (*http://www.wcc.nrcs.usda.gov/snotel/Wyoming/wyoming.html*) to collect snowpack and related climatic data in the Western United States (Wyoming) referred to as SNOTEL (i.e., SNOwpack TELemetry) (Figure 2 and Table 1). Monthly Snow Water Equivalent (SWE) values (inches) were obtained for the months of March, April, May and June. The monthly values were then summed to determine the total seasonal SWE and converted to centimeters. Unlike the streamflow data, a 40 year common period of record (1961 – 2000) was identified for all the SNOTEL stations. For each station, yearly water-year streamflow volumes (km^3) [or yearly total seasonal (March, April, May and June) SWE (cm)] were standardized (i.e., mean of zero and standard deviation of one).

PDO Index values are available from the Joint Institute for the Study of the Atmosphere and Ocean, University of Washington (*http://tao.atmos.washington.edu/pdo/*). For the period 1900 to present, the warm phase (1925 to 1945 and from 1977 to present) of the PDO Index was a positive numerical index value while the cold phase (1900 to 1925 and 1945 to 1977) was a negative numerical value (Mantua et al., 1997). A review of the PDO Index indicates a shift to the cold phase around 2000. McCabe et al. (2004) evaluated coupled effects of the PDO and the

Atlantic Multidecadal Oscillation. McCabe et al. (2004) assumed the PDO was in a warm phase from 1926 to 1943 and from1977 to 1994, and the PDO was in a cold phase from 1944 to 1976. The PDO phase periods used in the McCabe et al. (2004) study were adopted for this study with the assumption that the PDO shifts to the cold phase in 2000.

The NOAA-CDC (*http://www.cdc.noaa.gov/ENSO/Compare/*) defined the ENSO summer season as May to September and identified core El Niño and La Niña years for the summer season. The summer season was selected for ENSO since it was better represented by a season (e.g., an interannual oceanic / atmospheric phenomena). Various techniques were available to define the occurrence of a seasonal ENSO event (e.g., Gershunov, 1998; Hamlet and Lettenmaier, 1999; Harshburger et al., 2002; Rogers and Coleman, 2003]. When evaluating ENSO and PDO, Gershunov and Barnett (1998) defined a seasonal El Niño (La Niña) as when the anomaly in the Niño 3.4 sea surface temperature region (Trenberth, 1997) is greater (lesser) than 0.8 standard deviations of the long-term mean. They concluded that this value was high enough to exclude questionable ENSO events and would allow for an adequate number of ENSO events when combining the PDO (Gershunov and Barnett, 1998). For this study, the approach of Gershunov and Barnett (1998) was applied to the Niño 3.4 index and the Troup Southern Oscillation Index (*www.bom.gov.au*) for the summer (May to September) season and the results (summer season ENSO years identified) were used to compliment the NOAA-CDC core summer season ENSO year data set (i.e., recognize and incorporate additional ENSO years). This provides an adequate number of ENSO events to evaluate the impacts of the PDO while excluding questionable ENSO events (Gershunov and Barnett, 1998). Interdecadal and interannual climatic indices were evaluated one-year prior to streamflow and snowfall.

Methodology
First, spatial and temporal streamflow variability for the GRB and WBRB was evaluated by applying a 5-year filter to standardized water-year streamflow volumes for the two GRB stations and the three WBRB stations. Next, spatial and temporal snowfall (SWE) variability for the GRB and WBRB was evaluated by applying a 5-year filter to standardized seasonal SWE values for the four GRB stations and the three WBRB stations.

Finally, the impacts of the interdecadal (PDO) and interannual (ENSO) oceanic / atmospheric influences on WRR streamflow and snowfall were evaluated by testing of water-year (or seasonal) means for the individual and coupled oceanic / atmospheric influences.

The current water-year (October through September) was the period selected for streamflow and the spring season (March, April, May and June) was selected for SWE. The previous year (or season) was selected to define the phase (e.g., warm or cold) of the PDO and ENSO. This analysis evaluated the current water-year streamflow (or seasonal SWE) response (e.g., positive or negative shifts in means) to the previous year (or season) of the oceanic / atmospheric (PDO, ENSO) phase (cold or warm). The testing performed here was for both the individual and coupled oceanic / atmospheric indices with streamflow (or SWE).

The parametric two-sample t-test (Maidment, 1993) was performed on the response of streamflow means to changes in oceanic / atmospheric phase, including coupling. The t-test compares two independent data sets and determines if one data set has significantly larger values than the other data set (Maidment, 1993). The t-test assumes that the two data sets are normal

with equal variances (Maidment, 1993). A detailed discussion of this method is provided in Maidment (1993) and is also provided in most statistical textbooks.

Results
Spatial and Temporal Variability of Streamflow and SWE
The 5-year filter analysis resulted in stations (both GRB and WBRB) having similar spatial and temporal relationships (Figure 3a and 3b).

The period of record varied for the streamflow stations while a common period of record (1961 – 2000) was identified for the SNOTEL stations. While the late 1980's recession of Dinwoody Glacier (Pochop, et al. 1989) may be associated with deficit snowfall (Figure 3b), the continued recession, as identified in 1999 (Wolken, 2000) appears to coincide with normal, long-term (40 year period of record) snowfall (Figure 3b). The glacial recession may be a result of increased summer temperatures (ablation) in the region (Naftz et al., 2002).

Interestingly, for the 40 year period of record (1961-2000), the average seasonal SWE for the four GRB SNOTEL stations was 48.3 inches with a standard deviation of 17.8 inches. The average seasonal SWE for the three WBRB SNOTEL stations was 51.9 inches with a standard deviation of 15.2 inches. Therefore, snowfall amounts were virtually identical on each side of the continental divide.

Atmospheric-Oceanic Influences on Streamflow and SWE
Initially, the phases (cold and warm) were evaluated for the PDO and ENSO (individually) such that significant (greater than 90%) differences in streamflow (and SWE) means were reported. Next, the coupled impacts of the interdecadal PDO phases on La Niña (and El Niño) on streamflow (and SWE) means were evaluated.

The PDO signal (at 90% significance) was not detected in either streamflow or SWE. However, a significant ENSO signal was detected in three of five streamflow stations and all seven SWE stations. Figure 4 presents standardized seasonal SWE for La Niña and El Niño years. For all the SWE stations, the average standardized seasonal SWE after a previous summer season La Niña (El Niño) was +0.67 (-0.41). Neutral previous year summers resulted in average standardized seasonal SWE of -0.12. Therefore, a previous year summer La Niña (El Niño) results in increased (decreased) snowfall. Interestingly, the two streamflow stations (Dinwoody Creek – 06221400 and Bull Lake Crrek – 06224000) that failed to show an ENSO signal appear to have high contributions of glacial meltwater. This may explain why the ENSO signal was not identified in these streams.

Finally, an evaluation of the PDO's influence on ENSO was performed. For example, given the occurrence of a La Niña (or El Niño), how does the phase (cold or warm) of the PDO enhance (or dampen) the influence of La Niña (or El Niño) on streamflow (or SWE). The testing of PDO Cold – El Niño and PDO Warm – El Niño and, the testing of PDO Cold – La Niña and PDO Warm – La Niña for the streamflow stations resulted in no stations having a statistically significant difference in water-year streamflow.

The testing of PDO Cold – El Niño and PDO Warm – El Niño for the SWE stations resulted in no stations having a statistically significant difference in seasonal SWE. However, when testing PDO Cold – La Niña and PDO Warm – La Niña, three of the seven SWE stations were identified as having statistically significant differences in means (Figure 5). For all seven stations, the

average standardized seasonal SWE, given a previous summer season La Niña during a PDO Cold phase, was +1.09 while the average standardized seasonal SWE, given a previous summer season La Niña during a PDO Warm phase, was +0.04. Given that La Niña (i.e., ENSO cold phase) results in increased SWE, the PDO Cold phase enhances La Niña in this region. This is consistent with the findings of Gershunov and Barnett (1998) and Harshburger et al. (2002) that ENSO (El Niño or La Niña) is strongest during the similar PDO (warm or cold) phase.

Conclusions and Future Work
- Snowfall spatial and temporal variability (and average snowfall – SWE) were similar on each side (Green River Basin and Wind-Bighorn River Basin) of the continental divide.

- The PDO signal was not detected but a significant ENSO signal was detected in streamflow and SWE. A previous year summer La Niña (El Niño) results in increased (decreased) streamflow (or snowfall).

- The PDO Cold phase enhances La Niña in this region resulting in increased snowfall (SWE). Given a PDO Cold phase began on or about 2000, the development of a La Niña could result in above average snowfall.

- Future research will focus on extending the instrumental records (tree-ring reconstructions) of streamflow, SWE and temperature; evaluating Atlantic Ocean influences such as the Atlantic Multidecadal Oscillation and the North Atlantic Oscillation; and evaluating Pacific and Atlantic Ocean sea surface temperatures.

References
Beebee, R.A. and M. Manga (2004). Variation in the relationship between snowmelt runoff in Oregon and ENSO and PDO. *Journal American Water Resources Association*, 40(4), 1011-1024.
Gershunov, A. (1998). ENSO influence on influence on intraseasonal extreme rainfall and temperature frequencies in the contiguous United States: implications for long-range predicitability. *Journal of Climate*, 11, 3192-3203.
Gershunov, A., and T.P. Barnett (1998). Interdecal modulation of ENSO teleconnections. *Bulletin of the American Meteorological Society*, 79, 2715-2725.
Hamlet, A.F., and D.P. Lettenmaier (1999). Columbia River streamflow forecasting based on ENSO and PDO climate signals. *Journal of Water Resources Planning and Management*, 125(6), 333-341.
Harshburger, B., H. Ye, and J. Dzialoski (2002). Obervational evidence of the influence of Pacific sea surface temperatures on winter precipitation and spring stream discharge in Idaho. *Journal of Hydrology*, 264(1-4), 157-169.
Hidalgo, H.G. and J.A. Dracup (2003). ENSO and PDO effects on hydroclimatic variations of the Upper Colorado River Basin. *Journal of Hydrometeorology*, 4(1), 5-23.
Hidalgo, H.G. and J.A. Dracup (2001). Evidence of the signature of North Pacific multidecadal processes on precipitation and streamflow variations in the upper Colorado River Basin, *Proceedings of the 6th Biennial Conference of Research on the Colorado River Plateau*, United States Geological Survey, Arizona.
Maidment, D.R. (1993). *Handbook of Hydrology*. McGraw-Hill, New York, NY.

Mantua, N.J., S.R. Hare, Y. Zhang, J.M. Wallace, and R.C. Francis (1997). A Pacific interdecadal climate oscillation with impacts on salmon production. *Bulletin of the American Meteorological Society*, 78, 1069-1079.

McCabe, G.J., M.A. Palecki and J.L. Betancourt (2004). Pacific and Atlantic Ocean influences on multidecadal drought frequency in the United States. *PNAS*, 101(12), 4136-4141.

Meier, M.F. and A.S. Post (1962). Recent variations in mass net budgets of glaciers in western North America, In *Symposium on Variations of the Regime of Existing Glaciers*, Sept 10-18, Publication No. 58, International Association of Scientific Hydrology.

Naftz, D.L., D.D. Susong, P.F. Schuster, L.D. Cecil, M.D. Dettinger, R.L. Michel and C. Kendall (2002). Ice core evidence of rapid air temperature increases since 1960 in alpine areas of the Wind River Range, Wyoming, United States, *Journal of Geophysical Research*, 107(D13,4171).

Philander, S.G. (1990). *El Niño, La Niña and the Southern Oscillation*. Academic Press, Inc., San Diego, CA.

Pochop, L., R.A. Marston, G. Kerr, and M. Varuska (1989). *Long-term trends in glacier and snowmelt runoff, Wind River Range, Wyoming*. Project Report prepared for Wyoming Water Research Center, Laramie, WY.

Rogers, J.C. and J.S.M. Coleman (2003). Interactions between the Atlantic Multidecadal Oscillation, El Niño/La Niña, and the PNA in winter Mississippi Valley stream flow. *Geophysical Research Letters*, 30(10), 25-1-4.

Trenberth, K.E. (1997). The definition of El Niño. *Bulletin of the American Meteorological Society*, 78, 2271-2777.

Wallis, J.R., D.P. Lettenmaier, and E.F. Wood (1991). A daily hydroclimatological data set for the continental United States. *Water Resources Research*, 27(7), 1657-1663.

Wolken, G.J. (2000). *Energy balance and spatial distribution of net radiation on Dinwoody Glacier, Wind River Range, Wyoming, USA*. M.S. Thesis, Dept. of Geography and Recreation, University of Wyoming, May, 62 pp.
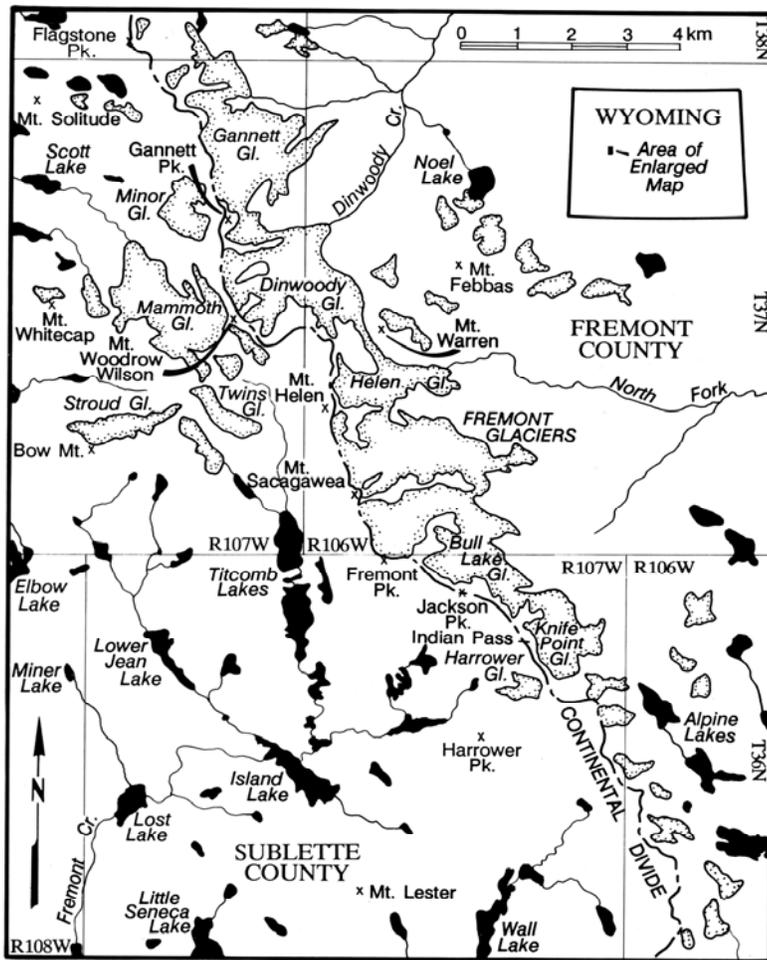
Figure 1:   **Area Map of Wind River Range Glaciers (Wolken, 2000).**
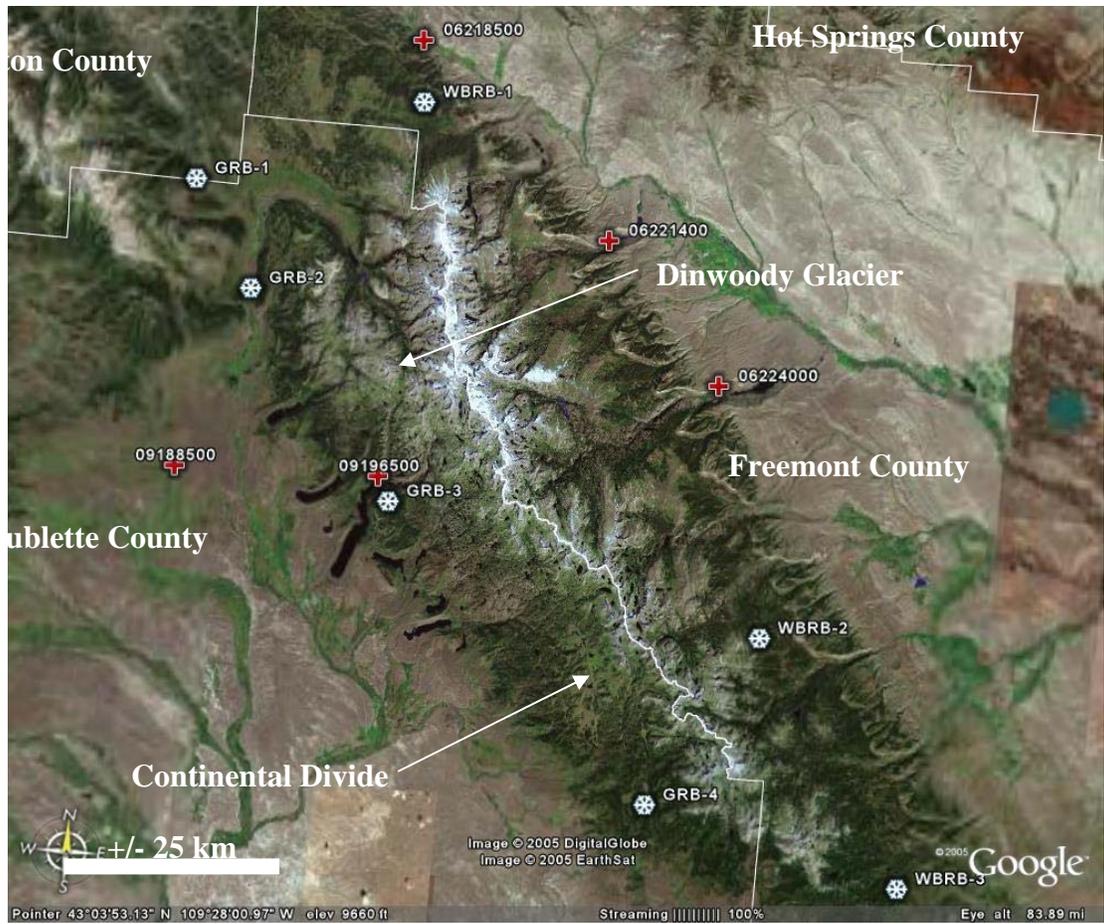
Figure 2: **Locations of unimpaired USGS streamflow stations and NRCS SNOTEL stations in the Wind River Range.**

(a)
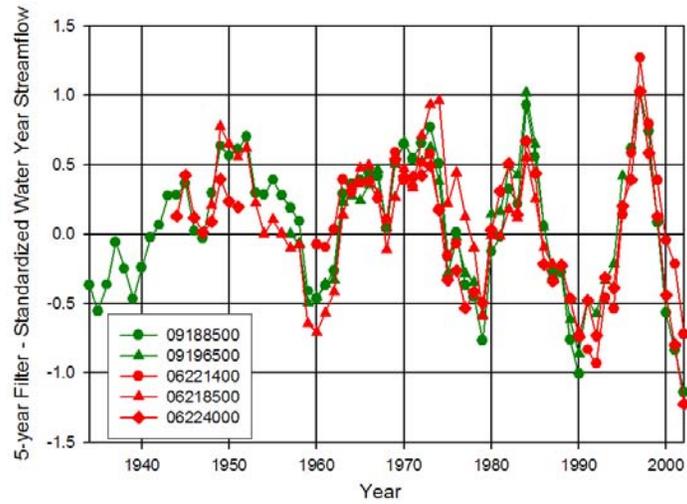
(b)
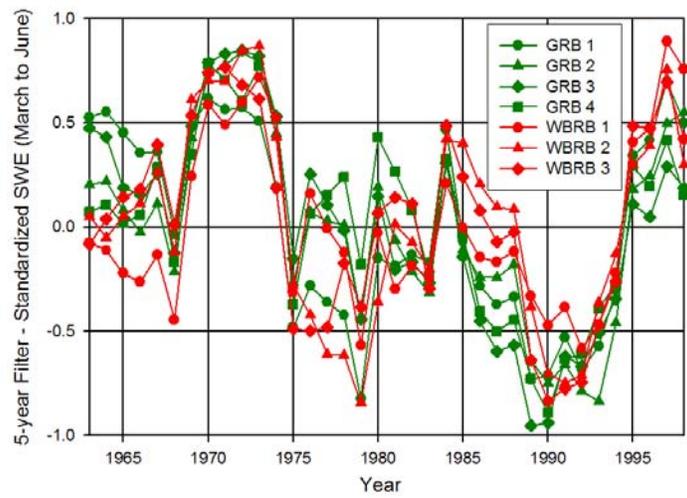
Figure 3: **5-year filter applied to Standardized (a) Water-year Streamflow (b) Seasonal SWE.**

Figure 4:   **Standardized seasonal SWE for La Niña (blue) and El Niño (red) years.**
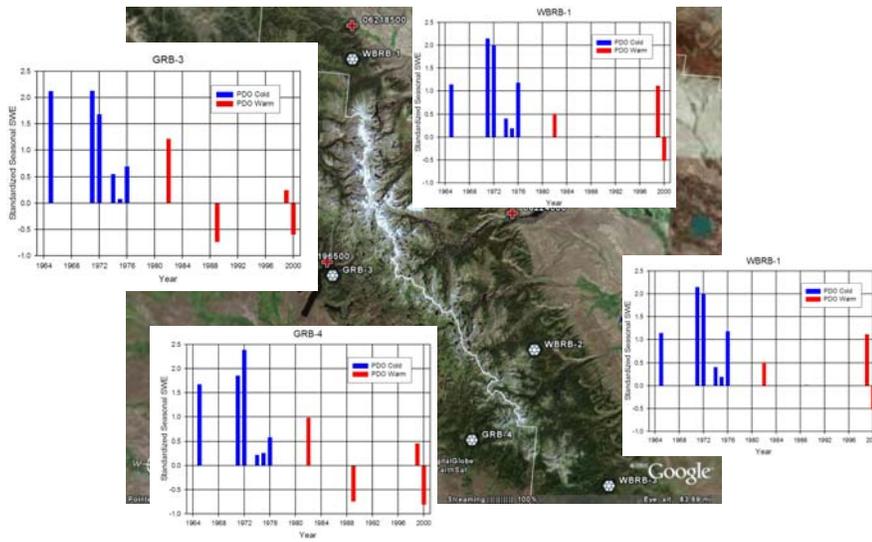
Figure 5: **Standardized seasonal SWE for PDO Cold (blue) and PDO Warm (red) for La Niña years.**

Table 1: **List of unimpaired USGS streamflow stations and NRCS SNOTEL stations in the Wind River Range.**

River Basin	Site Name	USGS or NRCS Site #	Latitude / Longitude
Green	Green River, Near Daniel, WY	09188500	43.02/-110.12
Green	Pine Creek Above Fremont Lake, WY	09196500	43.03/-109.77
Wind-Bighorn	Wind River Near Dubois, WY	06218500	43.58/-109.76
Wind-Bighorn	Dinwoody Creek, Near Burris, WY	06221400	43.35/-109.41
Wind-Bighorn	Bull Lake Creek Above Bull Lake, WY	06224000	43.18/-109.20
Green	Gros Ventre Summit, WY	506 (GRB-1)	43.39/-110.13
Green	Kendall R.S., WY	555 (GRB-2)	43.25/-110.02
Green	Elkhart Park G.S., WY	468 (GRB-3)	43.01/-109.76
Green	Big Sandy Opening, WY	342 (GRB-4)	42.65/-109.26
Wind-Bighorn	Little Warm, WY	585 (WBRB-1)	43.50/-109.75
Wind-Bighorn	Hobbs Park, WY	525 (WBRB-2)	42.87/-109.09
Wind-Bighorn	South Pass, WY	775 (WBRB-3)	42.57/-108.84